MASTERARBEIT | MASTER'S THESIS

Titel | Title

Towards the in-situ visualization of tRNA-derived small RNAs

verfasst von | submitted by

Diana Kokoric BSc

angestrebter akademischer Grad | in partial fulfilment of the requirements for the degree of

Master of Science (MSc)

Wien | Vienna, 2025

Studienkennzahl lt. Studienblatt | Degree programme code as it appears on the student record sheet:	UA 066 863
Studienrichtung lt. Studienblatt | Degree programme as it appears on the student record sheet:	Masterstudium Biologische Chemie
Betreut von | Supervisor:	Univ.-Prof. Dr. Stefan Ameres Dipl.-Biol. Univ.

Acknowledgements

First and foremost, this thesis would not have been possible without the generous support from Matthias Schaefer. I want to thank him for giving me the opportunity to conduct such an enriching research project in his group. He challenged me to develop new experimental skills and scientific knowledge that I will carry on beyond this thesis and into my future scientific pursuits. His guidance and feedback consistently motivated me to think independently and approach problems with curiosity.

A heartfelt thank you to my wonderful colleagues Nasim, Livia, Uliana, Victoria, and Emina, with whom I had the pleasure to work with. They all contributed to making our lab not just a great workplace, but an encouraging and enjoyable environment throughout this past year.

I am also deeply thankful for my family, whose continuous support and belief in me have been instrumental in helping me stay focused and motivated throughout my studies. And to my partner, David, your endless patience and understanding, especially during the most demanding phases of my studies, have been my anchor.

Abstract

The detection of tRNA-derived small RNAs (tsRNAs) is complicated by their size, their sequence, which is identical to their parental tRNAs, and the low ratio of tsRNAs/parental tRNAs. While methodologies such as hybridization chain-reaction (HCR) and rolling circle amplification (RCA) combined with fluorescent *in situ* hybridization (FISH) present promising potential for *in situ* signal amplification of tsRNAs, the greatest caveat is to distinguish the few tsRNAs from tRNAs with the same sequence information.
Building on previous attempts that utilized HCR for the detection of specific 5' tsRNAs during the oxidative stress response, which leveraged on exploiting the 3' cyclic phosphate (cycP) moiety, a distinct feature of 5' tsRNAs, this project aimed at overcoming a number of identified limitations in applying HCR to the problem of distinguishing tsRNAs from parental tRNAs. Specifically, new oligonucleotide probe designs for detecing tsRNAs and hybridzation conditions to optimize ligation efficiencies of probes were tested.
As a result, a hybrid RNA-DNA sequence formed by ligating a unique DNA probe to the 3' end of a specific tsRNA should serve as the landing site for a pad-lock probe design from which RCA can be initiated only at successfully ligated products. This work described the systematic testing and refining of the pad-lock probe hybridization and the amplification of pad-lock sequences *in vitro* as well as *in vivo* through applying the approach to the detection of ectopic tsRNAs in human somatic cells. Our aim is to particularly address the spurious background signal from parental tRNAs.

Zusammenfassung

Die Detektion von tRNA-abgeleiteten kleinen RNAs (tsRNAs) stellt eine besondere Herausforderung dar, da ihre geringe Größe, die identische Sequenz zu ihren parentalen tRNAs und das niedrige Verhältnis von tsRNAs zu parentalen tRNAs die spezifische Erfassung erschweren. Methoden wie die Hybridisierungs-Kettenreaktion (HCR) und die Rolling Circle Amplification (RCA) in Kombination mit Fluorescent *in situ* Hybridization (FISH) bieten vielversprechendes Potenzial zur *in situ*-Signalverstärkung von tsRNAs. Die größte Herausforderung besteht jedoch darin, die wenigen vorhandenen tsRNAs zuverlässig von ihren parentalen tRNAs mit derselben Sequenzinformation zu unterscheiden.
Aufbauend auf früheren Ansätzen, die HCR zur Detektion spezifischer 5'-tsRNAs während der oxidativen Stressantwort nutzten und dabei die 3'-zyklische Phosphatgruppe (cycP) als charakteristisches Merkmal von 5'-tsRNAs ausnutzten, zielte dieses Projekt darauf ab, bestehende methodische Limitationen zu überwinden. Insbesondere wurden neue Oligonukleotid-Sonden zur spezifischen tsRNA-Detektion entworfen und Hybridisierungsbedingungen optimiert, um die Ligationseffizienz der Sonden zu verbessern.
Eine zentrale Strategie bestand darin, eine hybride RNA-DNA-Sequenz zu erzeugen, indem eine spezifische DNA-Sonde an das 3'-Ende einer tsRNA ligiert wurde. Diese hybride Sequenz dient als Andockstelle für eine Padlock-Sonde, wodurch RCA ausschließlich an erfolgreich ligierten Produkten initiiert werden kann. Diese Arbeit beschreibt die systematische Optimierung der Padlock-Sonden-Hybridisierung sowie die Amplifikation der Padlock-Sequenzen *in vitro* und *in vivo* durch Anwendung des Ansatzes auf den Nachweis ektopischer tsRNAs in menschlichen somatischen Zellen. Ziel dieser Studie war es insbesondere, unspezifische Hintergrundsignale von parentalen tRNAs zu minimieren und eine hochsensitive sowie spezifische Methode zur Visualisierung von tsRNAs zu entwickeln.

List of Abbreviations

CL Complementary Linker

cycP 2',3'-cyclic phosphate

DNA Deoxyribonucleic Acid

Dox Doxycycline

FA formamide

FISH Fluorescence In Situ Hybridization

Gly Glycine

hANG human angiogenin

HCR Hybridization Chain Reaction

miRNA microRNA

PFA paraformaldehyde

R-LP RTCB-ligated platform

RCA Rolling Circle Amplification

RCP rolling circle product

RNA Ribonucleic Acid

RT room temperature

RT-PCR Reverse Transcription Polymerase Chain Reaction

ssDNA single-stranded DNA

tRNA transfer RNA

tsRNA tRNA-derived small RNA

Contents

1 Introduction

1.1 tRNA-derived small RNAs (tsRNA): A new class of small RNAs

Transfer RNAs (tRNAs) are the most evolutionarily conserved RNA molecules in all three main domains of life, as well as the most abundant RNAs in cells by number of molecules, besides ribosomal RNAs [1]. While the pivotal role of tRNAs in protein synthesis is a well-established fact, tRNAs are also the source of a heterogeneous class of small RNAs - tRNA-derived small RNAs (tsRNAs) [2].

Although tsRNAs are mostly associated with cellular stress responses, they are also present in non-stressed cells, suggesting a broader biological relevance. These RNA molecules have been detected in a range of physiological environments, including the hematopoietic system [3], various body fluids such as sperm, saliva, and urine [4], as well as extracellular vesicles [5].

Under conditions of cellular stress, mature tRNAs can undergo precise endonucleolytic cleavage at specific sites, a process that is highly conserved across different organisms [6, 7]. This cleavage commonly occurs in the anticodon loop and is catalyzed by anticodon nucleases (ACNases), leading to the formation of distinct 5' and 3' tRNA halves, typically between 31 to 40 nucleotides in length[8]. In mammalian cells, angiogenin, a member of the RNase A family, has been identified as a key enzyme mediating this process [7, 9]. Angiogenin cleavage generates tRNA halves with unique termini, such as a 5'-hydroxyl and a 2',3'-cyclic phosphate, which distinguishes them from mature tRNAs [10, 11].

Despite inconsistencies in nomenclature across different studies [8], the term tsRNAs will be consistently used throughout this thesis to describe RNA molecules derived from tRNA cleavage events, with a primary focus on 5' tRNA halves (5' tsRNAs).

1.2 Implications for tsRNAs as complexes with function

Recently, tsRNAs have gained increasing attention as potential regulatory molecules involved in a variety of cellular processes (reviewed in [8, 12]).

Various studies suggest that tsRNAs may act similarly to microRNAs (miRNAs) by binding to Argonaute proteins and influencing gene expression through post-transcriptional regulation [13–15]. Beyond gene regulation, tsRNAs have been linked to intergenerational inheritance. It was highlighted that intergenerational transmission of an acquired male phenotype could be mimicked by injecting sperm-derived RNA fragments into fertilized, wildtype oocytes [16]. Together with a previous finding that tRNA fragments are abundant in sperm [4], this association led to several emerging studies on the role of tsRNAs as an epigenetic factor [16, 17].

Despite these intriguing findings, one critical aspect that must be considered when interpreting the functional relevance of tsRNAs is the methodology used to establish their roles. Nearly all studies that associate tsRNAs with specific cellular processes relied on transfection experiments by which synthetic or *in vitro*-generated tsRNAs are introduced into cells in large quantities. These artificially high levels may not accurately reflect physiological conditions, potentially leading to exaggerated or even misleading conclusions about tsRNA function (reviewed in [8]). Given that endogenous tsRNA levels in cells are typically low and often fluctuate in response to stress or metabolic changes, their biological significance under normal conditions remains unclear.

Another key challenge is the lack of consistent detection methods for specific tsRNA species, especially at endogenous levels, which complicates efforts to distinguish their true biological impact from artifacts introduced by experimental conditions. Nonetheless, tsRNAs have shown considerable promise as biomarkers for disease diagnosis and monitoring [18]. Observed dysregulations of specific tsRNAs in cancer cells compared to normal cells have suggested their possible involvement in tumorigenesis [19–22]. Additionally, certain tsRNAs have been associated with other pathological conditions, including neurodegenerative disorders and metabolic diseases [23, 24]. However, much of this evidence stems from RNA sequencing (RNA-seq) data [11], a method that may introduce biases due to the extensive chemical modifications found in endo-

genous tRNAs and their sequences [25]. Given that modified bases potentially induce reverse transcription stops, RNA sequencing may not provide the most accurate picture of tsRNA abundance.

1.3 Detection of tsRNAs: Unveiling limitations and challenges

Clearly, previous studies made attempts to connect tsRNA function to various pathologic and physiologic states [3, 21, 24]. Detecting tsRNAs without sequencing, however, presents unique challenges due to their small size and their identical sequence to their parental tRNAs [26]. Classical detection methods for tsRNAs include RNA sequencing, Northern blotting, and microarray analysis [27]. While these methods are effective in quantifying tsRNAs in bulk, they fall short in elucidating the precise intracellular localization of these molecules.

1.3.1 Fluorescence *In Situ* Hybridization (FISH)

Fluorescence *in situ* hybridization (FISH) has been widely used to visualize RNA molecules within cells, but conventional FISH methods suffer from weak signal intensity for specific RNAs. This limitation arises because directly labeled complementary probes - whether fluorescent [28], radiolabeled [29], or chromogenic [30] - produce only a single detection signal per hybridized probe, potentially leading to insufficient sensitivity for detecting low-abundance RNA such as tsRNAs.

To improve FISH sensitivity, signal amplification approaches have been developed that enhance probe-based detection methods. Among them, Hybridization Chain Reaction (HCR) and Rolling Circle Amplification (RCA) have proven highly effective in increasing detection sensitivity for various RNA species [31].

1.3.2 Hybridization Chain Reaction (HCR)

HCR has been shown to significantly enhance the detection of both longer RNA molecules like messenger RNAs (mRNAs) [32, 33] and shorter ones like microRNAs (miRNAs) [31, 32].

Detecting miRNAs at the single-cell level presents similar challenges to tsRNA detection, primarily due to their short sequence length, which limits probe binding and detection sensitivity [32]. Additionally, miRNA families often contain closely related sequences, making specificity a key challenge [34]. To overcome these limitations, miRNA detection strategies have incorporated HCR-based amplification by designing complementary DNA probes linked to HCR initiator sequences. Upon hybridization to the target miRNA, these probes trigger a chain reaction, facilitating the sequential assembly of fluorescently labeled DNA hairpins into a polymeric structure at the binding site. This localized amplification dramatically enhances signal intensity, improving the visualization of low-abundance miRNAs [32].

Given its potential, HCR amplification was previously explored for the selective detection of 5' tsRNAs in somatic cells under oxidative stress [35], aiming to enhance FISH sensitivity for these low-abundance molecules. In this approach, a short, complementary RNA/DNA probe was designed to hybridize to the tsRNA and initiate the HCR cascade, leading to signal amplification. However, this method faced significant challenges in specificity, as background fluorescence from parental tRNAs interfered with tsRNA visualization. Additionally, secondary structures of tRNAs and tsRNAs likely hindered probe accessibility, necessitating further optimization of probe design and hybridization conditions.

1.3.3 Rolling Circle Amplification (RCA): A versatile tool

Another signal amplification method, Rolling Circle Amplification (RCA), has been used to further improve RNA detection sensitivity [31, 34, 36]. Unlike HCR, which relies on hybridization-based polymer formation, RCA uses a circularized DNA or RNA probe as a template for continuous strand elongation, generating long, single-stranded DNA (ssDNA) concatemers. Similar to FISH, RCA can incorporate different labeling strategies to generate detectable signals, either by incorporating fluorescently labeled nucleotides during elongation [37, 38] or by using fluorophore-labeled probes [36, 39].

A variant of the RCA approach has been developed to achieve ultrasensitive detection of microRNAs (miRNAs) in total RNA [34]. This method involves a padlock probe that hybridizes to a target miRNA and is subsequently ligated to form a circular DNA template. Once circularized, this template serves as the basis for RCA, continuously generating amplified DNA strands, that can be fluorescently detected.

One of the key advantages of this approach is its ability to amplify small RNA targets with high specificity while maintaining a relatively simple and isothermal amplification workflow. RCA, as employed in this study, is capable to generate extensive DNA amplification products, which significantly improve the signal-to-noise ratio when detecting low-abundance miRNAs , implying the potential application for biomarker identification in biomedical applications [31, 34].

2 Aims of the thesis

Building on first attempts of using fluorescent hybridization chain-reaction (HCR) methodology for the selective detection of specific 5' tsRNAs in somatic cells responding to oxidative stress (M.Sc. thesis Laura Borac), this project aimed at overcoming still existing limitations of the established method, mainly the spurious background signal from parental tRNAs, by using a modified signal amplification approach based on rolling circle amplification (RCA). More specifically, this M.Sc. thesis aimed at answering the following questions:

1. As tsRNA's sequence identity is identical to the tRNAs they derive from, can the 3' cyclic phosphate (cycP) feature of 5' tsRNAs be exploited to achieve selective detection?
2. And if so, can a methodology be developed that is based on creating a unique platform for selective signal amplification?
3. Is a RCA-based approach applicable for amplifying the *in-situ* detection signal of 5' tsRNAs in mammalian cells, and does this approach provide efficient and sufficient detection?

3 Experimental approach

A major challenge in visualizing tsRNAs is their low abundance, as only a fraction of tRNAs undergo cleavage under stress. To address this, synthetic fluorescently labeled 5' tsRNAs were introduced into cells via liposomal transfection, allowing controlled optimization of detection conditions before testing physiological stress-induced tsRNA formation.

Stress-induced cleavage in the anticodon loop generates 5' tsRNAs with a unique 2'-3' cyclic phosphate (cycP), a feature absent in mature tRNAs. This distinct 3' end was leveraged for sequence-specific ligation to a complementary linker (CL) using RTCB ligase, which selectively ligates cycP-containing RNAs to free hydroxyl groups.

To enable detection, this tsRNA-linker construct served as a template for padlock-probe circularization. RCA was then applied to amplify the signal, allowing for fluorescent detection and visualization using confocal microscopy.

4 Materials and Methods

Materials

Table 4.1: Buffers and Solutions

Buffer name	**Composition**
10x Phosphate Buffered Saline (PBS)	1.37 M NaCl 27 mM KCl 100 mM Na_2HPO_4 x $2H_2O$ 18 mM KH_2PO_4
5x Tris-Borate buffer (TB)	446 mM Tris base 445 mM ortho-boric acid
1x Tris-EDTA buffer (TE)	10 mM Tris-HCl 1 mM EDTA
1x Tris-Acetate-EDTA buffer (TAE)	40 mM Tris-Acetate 1 mM EDTA
10x M-MuLV Buffer	500 mM Tris-HCl 750 mM KCl 30 mM $MgCl_2$ 100 mM DTT
10x RTCB Buffer	500 mM Tris-HCl 750 mM KCl 30 mM $MgCl_2$ 100 mM DTT
5x GoTaq Green Reaction Buffer	1 mM dNTPs 7.5 mM $MgCl_2$
10x CutSmart Buffer	500 mM Potassium Acetate 200 mM Tris-Acetate 100 mM Magnesium Acetate 1 mg/ml BSA
1x Proteine Extraction Buffer	1x RIPA 5 mM DTT 1x PIC

5x T4 DNA Ligase Reaction Buffer	250 mM Tris-HCl (pH 7.6) 50 mM $MgCl_2$ 5 mM ATP 5 mM DTT 25% (w/v) polyethylene glycol-8000
10x Φ29 DNA Polymerase Buffer	500 mM Tris-HCl 100 mM $MgCl_2$ 100 mM $(NH_4)_2SO_4$ 40 mM DTT
1x Transfer Buffer	1x Borate Buffer 20% Methanol 1 mM DTT 2 mM EDTA
PBS-T	1x PBS 0.05% Tween
RNA extraction buffer	0.3 M NaOAc 0.1 % SDS 1 mM EDTA
2x RNA loading dye	77.5% Formamide 0.025% SDS 0.025% bromophenol blue 0.025% Xylene Cyanol 0.025% EtBr 5 mM EDTA
20x Saline sodium citrate (SSC)	3 M NaCl 300 mM sodium citrate
15% FA hybridization solution	5x SSC 100 µg/µl Heparin 1x Denhardt's Reagent 0.1% Tween 20 0.1% CHAPS 5 mM EDTA 15% Formamide

20% FA hybridization solution	1x T4 DNA ligase reaction buffer 0.05 mM KCl 0.2 µg/µl BSA 20% Formamide
10% FA hybridization solution	6x SSC 10% Formamide
Blocking buffer	3% BSA 0.05% NaN_3 0.1% TritonX-100 1x PBS
Northern-Hybridization Buffer	5x SSC 20 mM Na_2HPO_4 (pH 7.4) 7% SDS 1x Denhardt's Reagent

Table 4.2: Chemicals

Chemicals	**Supplier**
Acetic acid	Labochem (LC-10045.1)
Bovine serum albumin (BSA)	Sigma-Aldrich (A9418)
Bromphenol blue	VWR (0449)
Chloroform ($CHCl_3$)	Chem-Lab (CL0003162500)
Dithiotreitol (DTT)	PanReac (A1101)
Doxycycline (Dox)	Sigma-Aldrich (564-25-0)
Ethanol (96 %) (EtOH)	Chem-Lab (CL00.0507.5000)
Ethylene diamine tetraacetate (EDTA)	Panreac (A1103.1000)
Formamide (CH_3NO)	Sigma (47671)
Guanosine triphosphate (GTP)	New England Biolabs (N2080A)
Glycerol 87%	Panreac (A0970.5000)
Glyoxale 40%	Sigma-Aldrich (50649)
Hydrochloric acid (HCl)	Carl Roth (19251)
Magnesium chloride ($MgCl_2$)	Sigma-Aldrich (M8266)
Mangane chloride ($MnCl_2$)	New England Biolabs (B1761S)
Methanol (CH_3OH)	VWR (20903.368)
Milk powder	Maresi
Paraformaldehyde (PFA)	Sigma-Aldrich (P6148)
Polyethylenglykol (PEG) 8000	Carl Roth (0263.1)
Polyacrylamide (39:1) (Rotiphorese® Gel 40)	Carl Roth (3030.2)
Roti-Phenol	Carl Roth (0038.2)
Sodium acetate (NaOAc)	Sigma-Aldrich (241245)
Sodium azide (NaN_3)	Sigma-Aldrich (71290)
Sodium citrate ($Na_3C_6H_5O_7$)	Gerbu (6132-04-3)
Sodium chloride (NaCl)	Panreac (A2942.5000)
Sodium dodecyl sulfate (SDS)	Carl Roth (8029.3)
Sodium hydroxide (NaOH)	Panreac (131687)
Tetramethylethylendiamine (TEMED)	Panreac (A1148.0025)
Tris-HCl	VWR (MOLE14689173)

Table 4.3: Cell Culture Reagents

Product	**Supplier**
Dulbecco's Modified Eagle Medium (DMEM)	Thermo Fisher Scientific (11960044)
Fetal Bovine Serum (FBS)	Thermo Fisher Scientific (10500-064)
L-Glutamine	Sigma-Aldrich (G8540-25)
Penicillin-Streptomycin	Thermo Fisher Scientific (15140122)
Lipofectamine™ 2000 transfection reagent	Thermo Fisher Scientific (11668019)
Opti-MEM™ reduced serum medium	Gibco (10149832)

Table 4.4: Other materials

Material	**Supplier**
Agarose	LABQ (LQ1630440500)
Aminoallyl-dUTP-XX-ATTO-488	Jena Bioscience (NU-803-XX-488)
ExpressLink™ T4 DNA Ligase	Thermo Fisher Scientific (11370862)
GoTaq DNA Polymerase	Promega (M300A)
innuPREP Plasmid Mini Kit	Analytik Jena (845-KS-5041050)
LB agar	PanReac (A0949.500)
Microscopy chamber slides	Thermo Fisher Scientific (12-565-1)
Microspin S-300 HR columns	Sigma-Aldrich (GE27-5130-01)
Microspin P-6DG columns	BioRad (7326201)
Mix2Seq Kit NightXpress	Eurofins
M-MuLV Reverse Transcriptase	Thermo Fisher Scientific (28025013)
Nanosep columns	Pall Corporation (ODM45C34)
Nylon blotting membrane	Cytiva (RPN203B)
Φ29 DNA Polymerase	New England Biolabs (M0269L)
pCR®2.1 vector (25 ng/µl)	Thermo Fisher Scientific (K202020)
Rnase Inhibitor	Thermo Fisher Scientific (N8080119)
RTCB Ligase	New England Biolabs (M0458S)
ROTI®Mount FluorCare	Carl Roth (HP19.1)
Streptavidin-coated beads	Thermo Fisher Scientific (65001)

4.1 Oligonucleotide Probe Designs

All oligonucleotides used in the present work were purchased from either Biomers (Ulm, Germany) or Sigma-Aldrich (Darmstadt, Germany). RNAfold was used for probe designs, to predict any secondary structure. All oligonucleotide sequences can be found in Table 4.5.

4.1.1 RTCB-mediated Ligation

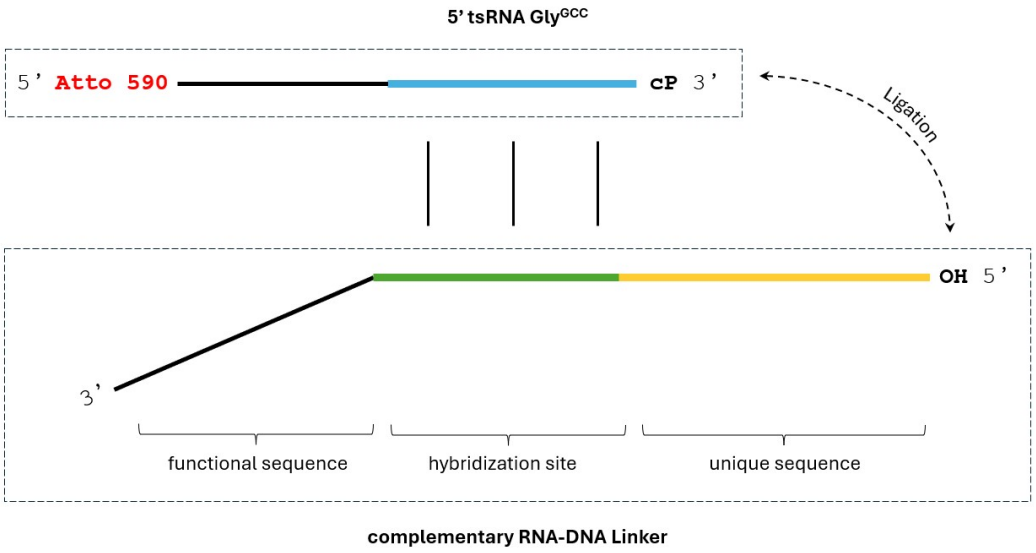

Figure 4.1: Complementary linker design for RTCB-mediated ligation of a 5' tsRNA and a DNA linker.
(blue) Region of 5' tsRNA Gly^{GCC} complementary to linker. (green) Region of linker complementary to the 5' tsRNA Gly^{GCC}. (yellow) Region of linker, which together with the blue region of 5' tsRNA is forming the RTCB-ligated platform in its closed conformation via RTCB-mediated ligation. (red) Atto590 fluorophore at the 5' end of the 5' tsRNA. cP: 2',3'-cyclic phosphate at the 3' end of the 5' tsRNA. OH: hydroxyl group at the 5' end of the linker. Vertical lines indicate hybridization between the 5' tsRNA Gly^{GCC} and the complementary RNA/DNA linker. Sequences summarized in Table 4.5

Different complementary linkers (or CLs) of 52 to 64 nucleotide length were designed to be specific to the 3' end of the 5' tsRNA-Gly^{GCC}. RTCB-mediated ligation reactions were performed on a synthetic 5' tsRNA-Gly^{GCC} template. The hybridization site was designed in a way that complementary sequence length could be tested for RTCB-mediated ligation efficiency. All probes designed carried two ribonucleotides at their 5' end. The 5' hydroxyl group of the CL and the 3' cycP of the target tsRNA are required for RTCB ligation.

At the 3' end, CLs carried a 20 nucleotide-long overhang with an functional sequence that does not naturally occur in cells. This terminal overhang served as a landing site for a toehold probe, mediating the opening of the secondary structure of the ligation product formed between the 5' tsRNA-Gly^{GCC} and the CL, as a prerequisite for padlock probe hybridization and RCA.

At the 5' end, CLs harbored an additional sequence of 17 nucleotide length, which was not complementary to the 5' tsRNA-Gly^{GCC} in order to form a loop upon hybridization and RTCB-mediated ligation. Upon opening of the secondary structure of the ligation product, a unique sequence is generated, which was called split-landing site.

4.1.2 RCA-based Detection

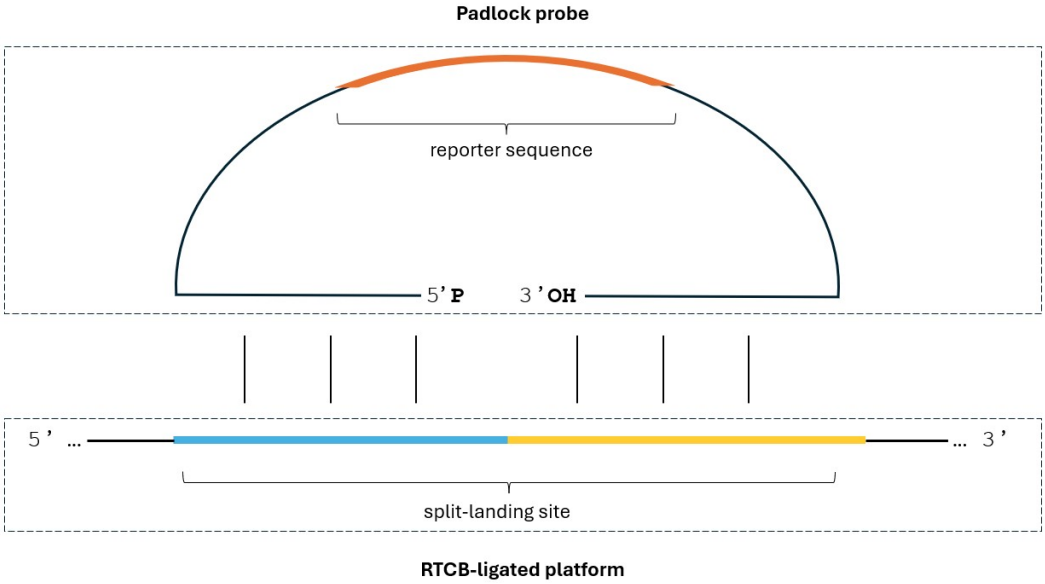

Figure 4.2: Padlock probe design for RCA-based detection on a RTCB-ligated 5' tsRNA-DNA hybrid.
(orange) Reporter sequence within the padlock probe used for RCA product detection. Split-landing site within the RTCB-ligated platform formed between (blue) region of the 5' tsRNA Gly^{GCC} and (yellow) region of the complementary RNA/DNA linker. P: phosphate group at the 5' end of the padlock probe. OH: hydroxyl group at the 3' end of the padlock probe. Vertical lines indicate hybridization between the split-landing site and the 5' and 3' end of the padlock probe. Sequences summarized in Table 4.5

The padlock probe was designed such that upon hybridization to the split landing site, it undergoes circularization forming a nick between terminal arms. The arms of the padlock probe of 18 nucleotide length were designed in such a way that one arm would hybridize specifically to the 5' tsRNA moiety while

the other arm would hybridize to the (at this stage) unfolded CL. Only in cases where the padlock correctly hybridized to the RTCB-ligated platform (or R-LP), the platform would provide the exact sequence for loop-closing ligation mediated by T4 DNA ligase. For detection of rolling circle products (RCP) a reporter sequence was embedded in the sequence, which was linked by a poly(A) sequence to the probe arms.

Table 4.5: Oligonucleotides

Oligonucleotide	Sequence (5'-3')[a]	Length	3' end	5' end	Identity	Application	Purpose
AD137	GCA UGG GUG GUU CAG UGG UAG AAU UCU CGC CU	32	cycP	Atto 590	RNA	general	5' tsRNA-Gly^{GCC}
DK004	rGrGC TGT AGG CAC CAT CAA T**AG GCG AGA ATT CTA CCA CTG AAC C**AG ATC GGA AGA GCA CAC GTC T	64	Spacer C3	-	RNA/DNA	general	complementary to 5' tsRNA-Gly^{GCC}
DK005	rGrGC TGT AGG CAC CAT CAA T**AG GCG AGA ATT CTA CCA C**AG ATC GGA AGA GCA CAC GTC T	58	Spacer C3	-	RNA/DNA	general	complementary to 5' tsRNA-Gly^{GCC}
DK006	rGrGC TGT AGG CAC CAT CAA T**AG GCG AGA ATT C**AG ATC GGA AGA GCA CAC GTC T	52	Spacer C3	-	RNA/DNA	general	complementary to 5' tsRNA-Gly^{GCC}
DK008	rGrGC TGT AGG CAC CAT CAA T**AG GCG AGA ATT CTA CCA C**AG ATC GGA AGA GCA CAC GTC T	58	Biotin-TEG	-	RNA/DNA	RCA	complementary to 5' tsRNA-Gly^{GCC}
DK009	<u>AGG CGA GAA TTC TAC CAC</u> AAA AAA AAA AAA **AGT AGC CGT GAC TAT CGA CT** AAA AAA AAA AAA <u>TTG ATG GTG CCT ACA GCC</u>	80	-	Phosphate	DNA	RCA	Padlock probe
DK012N	AGT AGC CGT GAC TAT CGA CT	18	-	Atto488	DNA	RCA	Detector probe
DK013	GTG GTA GAA TTC TCG CCT GGC TGT AGG CAC CAT CAA	36	-	-	DNA	RCA	Split-landing site

[a] Underlined: Complementary sequence to the RNA or DNA target; Bold: Detection probe and RCA primer hybridization site.

Oligonucleotide	**Sequence (5'-3')**[a]	**Length**	**3' end**	**5' end**	**Identity**	**Application**	**Purpose**
DK014	GTG GTA GAA TTC TCG CCT GGC TGT AGG CAC CAT CAA	36	Biotin-TEG	-	DNA	RCA	Split-landing site
DK015	AGA CGT GTG CTC TTC CGA TCT GTG GTA GAA TTC TCG CCT	39	-	-	DNA	RCA	Toehold probe
DK016	ATT GAT GGT GCC TAC AGC C	19	-	-	DNA	RT-PCR	Primer
DK017	ATT GAT GGT GCC TAC AGC CAG	21	-	-	DNA	RT-PCR	Primer
DK018	TAG CCG TGA CTA TCG ACT	18	-	-	DNA	RCA	Northern Blot
DK018N	AGT CGA TAG TCA CGG CTA	18	-	-	DNA	RCA	RCA Primer
DK019	GTG GTA GAA TTC TCG CCT GGC TGT AGG CAC CAT CAA	36	-	Atto565	DNA	RCA	Split-landing site
DK020	<u>AGG CGA GAA TTC TAC CAC</u> AAA AAA AAA AAA **AGT AGC CGT GAC TAT***[FlcdT] **CGA CT** AAA AAA AAA AAA <u>TTG ATG GTG CCT ACA GCC</u>	80	-	Phosphate	DNA	RCA	Padlock probe
DK021	rGrGC TGT AGG CAC CAT CAA T**AG GCG AGA ATT CTA CCA C**AG ATC GGA AGA GCA CAC GTC T	58	Spacer C3	Atto488	RNA/DNA	general	complementary to 5' tsRNA-Gly^{GCC}
M13 fwd.	GTA AAA CGA CGG CCA G	16	-	-	DNA	Cloning	forward primer
M13 rev.	CAG GAA ACA GCT ATG AC	17	-	-	DNA	Cloning	reverse primer
MattVIE418	GCA TGG GTG GTT CAG TGG	18	-	-	DNA	RT-PCR	Primer
MattVIE426	rGrGC AGG CGA GAA TTC TAC CAC TGA ACC ACC CAT GCA ACT GTA GGC ACC ATC AAT GGC	57	Spacer C3	-	RNA/DNA	general	complementary to 5' tsRNA-Gly^{GCC}

[a] Underlined: Complementary sequence to the RNA or DNA target; Bold: Detection probe and RCA primer hybridization site.

Methods

4.2 General Cell Culture Methods

Cultured Cell Lines

HeLa and HEK293 cells were cultured in Dulbecco's Modified Eagle's Medium (DMEM) supplemented with 10% FBS (v/v), 2 mM L-Glutamine, 100 U/ml penicillin and 100 µg/ml streptomycin (DMEM+F/G/P/S). The cells were maintained in a humidified incubator at 37°C and 5% CO2.

Propagation of Cell Lines

Medium was removed and cells were washed with 1x DPBS. 1x Trypsin/EDTA was added to cells (1.5 ml per 10 cm ⌀ dish) followed by incubation for two minutes at 37°C and 5% CO_2. To stop the trypsinization, DMEM+F/G/P/S was added and cells were collected. To maintain and propagate each cell line, a near confluent dish was split at a ratio of 1:20 every four days.

Liposomal Transfection

HeLa cells grown in microscopy chamber slides were allowed to reach approximately 70-80% confluency before transfection. Oligonucleotides (150 ng or as indicated) were diluted in Opti-MEM reduced serum medium. A transfection mixture was then prepared using Lipofectamine 3000, following the manufacturer's protocol. The existing culture medium was exchanged for 200 µl of Opti-MEM, and after a 10-20 minute incubation period, the transfection mix was added. Cells were incubated overnight at 37°C.

Ectopic expression of hANG

The ectopic hANG cell line is a previously established HEK293 model engineered to express human Angiogenin (hANG) with HA and FLAG tags under an inducible promoter [40]. When cells reached 70-80% confluency, hANG-HA-FLAG expression was induced by adding 0.2 g/ml doxycycline (Dox) to the culture medium. Cells were maintained in the presence of Dox for three days.

4.3 General Nucleic Acids Methods

Phenol Extraction

Extraction began with the addition of 750 µl of Roti-Phenol to the sample, followed by thorough mixing and incubation at RT for 30 minutes. Subsequently, an equal volume of 1× TE buffer was added, and the mixture was centrifuged at 5 000 x g for 10 minutes at 4°C to separate phases. The upper aqueous phase was collected, and an equal volume of chloroform was added. After thorough mixing, the sample was centrifuged again under the same conditions. The resulting upper aqueous phase was transferred to a fresh 1.5 ml Eppendorf tube. To this, 0.1 volumes of 3 M NaOAc (pH 5.0), one volume of isopropanol, and 1 µl of glycogen (µl/ml) were added. Following a short spin, the sample was incubated overnight at 4°C to precipitate nucleic acids. On the next day, the suspension was centrifuged at 21 000 x g for 30 minutes at 4°C. The precipitate was washed with 75% ethanol, followed by centrifugation for 5 minutes under the same conditions. The pellet was air-dried for 5 minutes, and resuspended in 10 µl of nuclease-free water.

Gel Purification

RTCB ligation products were extracted from denaturing 15% urea-PAGE gels. After electrophoresis, the ligation products were visualized under a short-wavelength UV lamp, and the corresponding gel slices were excised. To extract the product, 800 µl of RNA extraction buffer was added to the gel slices, and the mixture was rotated at 4°C overnight. The suspension was centrifuged at 21 000 x g for 5 minutes at RT, and the supernatant was carefully transferred to nanosep columns, avoiding acrylamide contamination. The sample was centrifuged at 1000 x g for 1 minute at RT, and the eluate was collected into a fresh Eppendorf tube. The total volume was determined, and 0.1 volumes of 3 M NaOAc (pH 5.0), one volume of isopropanol, and 1 µ of glycogen (µl/ml) were added. After mixing, the sample was incubated at RT for at least 45 minutes or overnight at 4°C to facilitate precipitation. The precipitate was collected by centrifugation at 4°C for 30 minutes at 21 000 x g, followed by washing with 75% ethanol containing 5 mM $MgCl_2$. The sample was centrifuged again for 5 minutes under the same conditions, and the ethanol was removed. The pellet was air-dried for 5 minutes and resuspended in 10 µl of nuclease-free water.

Reverse transcription PCR

Cross-validation of RTCB-mediated ligation was carried out by RT-PCR. Ligation products were used directly after incubation with RTCB or extracted from gel. For this step, the ligation products were identified as a SYBR gold positive signal of expected molecular size, excised from an urea-PA gel, shredded, and eluted with 800 µl RNA extraction buffer at 4°C overnight on a spinning wheel. The ligation products that were used directly after RTCB-mediated ligation were purified with Microspin S-300 HR columns following the manufacturer's instructions. RNA/DNA extraction and precipitation was performed as described before.

Next, cDNA synthesis targeting the junction region of the RTCB-ligated platform was performed. To this end, RTCB ligation products were mixed with a primer, dNTPs and water according to Table 4.6. Samples were denatured for 3 minutes at 80°C and put on ice promptly. Afterwards, the remaining reagents were added and the reaction was incubated for 5 minutes at 25°C, then one hour at 42°C, followed by inactivation of the RT enzyme for 15 minutes at 75°C. The cDNA was stored at 12°C overnight or until use.

Table 4.6: Reverse transcription reaction mixture

Reagent	**Volume [µl]**
Ligation product (5 ng/µl)	1
RT primer DK017 (1 µM)	2
dNTPs (10 mM)	1
Water	up to 10
10x M-MuLV buffer	2
M-MuLV RT (200 U/µl)	1
RNase inhibitor (40 U/µl)	0.2
Water	6.8
Total	20

Only a fraction of the reverse transcription reaction was used for amplification by PCR. The reverse transcription product was amplified in the following reaction mix (Table 4.7) using a standard PCR program: denaturation at 94°C for 3 minutes, 30 cycles of template denaturation at 94°C for 15 seconds, primer annealing at 58°C for 30 seconds, extension at 72°C for 15 seconds, final

extension at 72°C for 5 minutes, hold at 4°C.

Table 4.7: PCR mixture

Reagent	**Volume [µl]**
cDNA	2.5
5x GoTaq green reaction buffer (10 µM)	5
dNTPs (10 mM)	1
forward primer MattVIE418 (10 µM)	0.5
reverse primer DK016 (10 µM)	0.5
GoTaq polymerase (5 U/µl)	0.5
Water	15
Total	25

Southern blotting

RCA products were seperated on 0.5% agarose gels in 1x TAE and stained with SYBR green. The DNA was transferred onto nylon membranes using two methods:

Vacuum Blotting

After electrophoresis, the gel was denatured in a solution of 1.5 M NaCl and 0.5 M NaOH for 30 minutes. Following that, the gel was neutralized in 1.5 M NaCl and 0.5 M Tris-HCl (pH 7.4) for another 30 minutes. The DNA was subsequently transferred onto a nylon membrane using vacuum blotting with 10x SSC buffer at 0.25 bar for 90 minutes.

Capillary Blotting

Prior to transfer, the gel was incubated in 0.25 M HCl for 15 minutes to depurinate the DNA, followed by denaturation in 0.6 M NaCl, 0.4 M NaOH for 30 minutes. After rinsing, the gel was neutralized in 1.5 M NaCl, 0.5 M Tris-HCl (pH 7.4) for 30 minutes. Transfer was performed through upward capillary blotting using 10x SSC as the transfer buffer. The blotting was carried out over 20 hours to ensure complete transfer via capillary action. Afterwards, the nylon membrane was incubated in 0.4 M NaOH (1 minute) and in 0.2 M Tris-HCl pH 7.4 (1 minute).

Post-transfer, blotted DNA was cross-linked using UV at 120 mJ/cm^2 (UVP

Crosslinker CX-2000, Analytik Jena), followed by incubation of the membrane at 60°C overnight to ensure immobilization.

Radioactive labeling and Hybridization

Radioactive labeling experiments were performed with the help of Matthias Schaefer. The nylon membrane with immobilized DNA was pre-hybridized in Northern hybridization buffer for one hour at 39°C. For visualization, complementary oligonucleotides (DK018) targeting the recognition site of the amplicons were radioactively labeled using T4 PNK forward reaction and p^{32}-γ-ATP (Table 4.8). The reaction proceeded at 37°C for one hour and was inactivated by heating at 75°C for 5 minutes. Post-reaction, the labeled probes were diluted with 50 µl of water and unincorporated p^{32}-γ-ATP were removed by desalting using Bio-Rad Microspin-columns with P-6DG polyacrylamide gel. These purified probes were then added to the Northern hybridization buffer and incubated overnight at 39°C.

Table 4.8: Radioactive labeling of oligonucleotides

Reagent	**Volume [µl]**
DK018 (10 µM)	0.5
T4 Polynucleotide kinase (10 µM)	2
10x T4 Polynucleotide kinase buffer A	1
p^{32}-γ-ATP (10 mCi/ml)	0.5
Water	16
Total	20

After the hybridization, membranes were washed with 3x SSC, 5% SDS at 39°C for 15 minutes, followed by 1x SSC, 1% SDS at RT for 15 minutes. Washed membranes were exposed to a phospho-imaging screen (GE healthcare) at RT and developed using an Amersham Typhoon Biomolecular Imager (GE healthcare).

4.4 General Molecular Cloning Methods

Topoisomerase based cloning

To set up the TOPO cloning reaction, a 3:1 ratio of PCR product to linearized vector was used.

PCR product was ligated into the pCR2.1 TOPO vector with T4 DNA ligase in 1x T4 DNA ligase buffer for 25 minutes at RT. Competent *E. coli* cells were thawed on ice for 10 minutes. Ligation mix was added to the cells and then left on ice for another 10 minutes. Heat-shock transformation was done at 37°C for 5 minutes and subsequently cooled on ice for 1 minute. Transformed cells were recovered in 400 µl S.O.C. media for 30 minutes at 37°C. After centrifugation at 1000 x g for 1 minute, the supernatant was reduced to 70 µl. The suspension was plated on plates with selective media to allow expression of antibiotic resistance markers and isolate colonies containing the cloned DNA fragment.

After incubation overnight at 37°C, colony PCR was performed to identify positive clones with primers (M13 fwd and M13 rev) annealing to the plasmid. Selected colonies were grown in LB medium with ampicillin and an innuPREP Plasmid Mini Kit was further used to isolate the plasmids. Mix2seq kit tubes were used to mix the isolated plasmid with the forward primer and samples were Sanger sequenced by Eurofins. Analysis of the sequencing results was performed with Serial Cloner 2.6.1.

4.5 General Protein Methods

Expression and Purification of His_6-tagged RTCB

First ligation tests were performed using commercially available human His-tagged RTCB ligase from recombinant expression in *E. coli*. Later ligations were carried out using recombinant RTCB that was expressed in house followed by purification with the help of Victoria Guggenberger and Nasim Sanadgol. Through a combination of Ni-NTA affinity chromatography, and Superdex $200_{10/300}$ SEC columns, purified RTCB with a calculated concentration of 1.125 mg/ml based on molecular absorption coefficients. The purified protein was analyzed by SDS-PAGE and the presence of the His-tag was confirmed using Western blotting with anti-HA antibodies.

The enzyme activity and ligation efficiency of the recombinantly expressed RTCB was assessed in different concentration and compared to commercially available RTCB in ligation reactions using synthetic 5' tsRNA-Gly^{GCC} and the chosen CL. It is important to note that the RTCB ligase used in the initial *in vitro* experiments - such as testing ligation time and enzyme concentration - had a concentration of 0.318 mg/ml. Therefore, the volume of the ligase added was adjusted accordingly to achieve equimolar concentrations when compared

with later ligation reaction. Activity of recombinant human RTCB as well as in combination with human His-tagged Archease (provided by Peschek lab, Heidelberg University, Heidelberg) was tested by *in vitro* ligation of the 5' tsRNA-Gly^{GCC} and the chosen CL.

Immunostaining of recombinant human RTCB

After fixation and permeabilization, cells were incubated with 5 µl of recombinant human RTCB (24.9 µM) for 2 hours at 37°C. Post-fixation using 4% PFA was followed by brief washing with blocking buffer. Next, 200 µl of blocking buffer was added and incubated for 30 minutes at RT. The blocking buffer was then replaced with 200 µl of primary antibody provided by Isabella Moll, MPL, Vienna (rabbit anti-RTCB, 1:1000 in blocking buffer), and cells were incubated overnight at 4°C in a humidified chamber.

The following day, cells were washed twice briefly in blocking buffer, followed by incubation with the secondary antibody (goat anti-rabbit Alexa 488, 1:500 in blocking buffer) for 2 hours at RT. Cells were washed three times for 5 minutes each with 1× PBS and stained with Hoechst (1:5000 in PBS) for 5 minutes. After a final brief wash, cells were mounted and sealed with a glass coverslip before imaging.

4.6 Overview of the Method Flow

The experimental design aimed to develop a robust methodology for *in-situ* detection of 5' tsRNAs in mammalian cells, integrating RTCB-mediated ligation with Rolling Circle Amplification (RCA) to enhance detection sensitivity. As depicted in Figure 4.3, an *in vitro* approach using a synthetic 5' tsRNA-Gly^{GCC}, fluorescently labeled at its 5' end, was first established to optimize each step (❶-❼) of the detection workflow before transitioning to the more complex cellular environment. Previously optimized parameters served as the starting point for each successive optimization.

❶ Hybridization of Complementary Linker (CL): The linker was annealed to the 3' end of the 5' tsRNA under optimized hybridization conditions, creating a stable platform for subsequent ligation.

❷ RTCB-Mediated Ligation: RTCB ligase facilitated the loop-closing ligation, forming the RTCB-ligated platform (R-LP) with a hairpin conformation. This

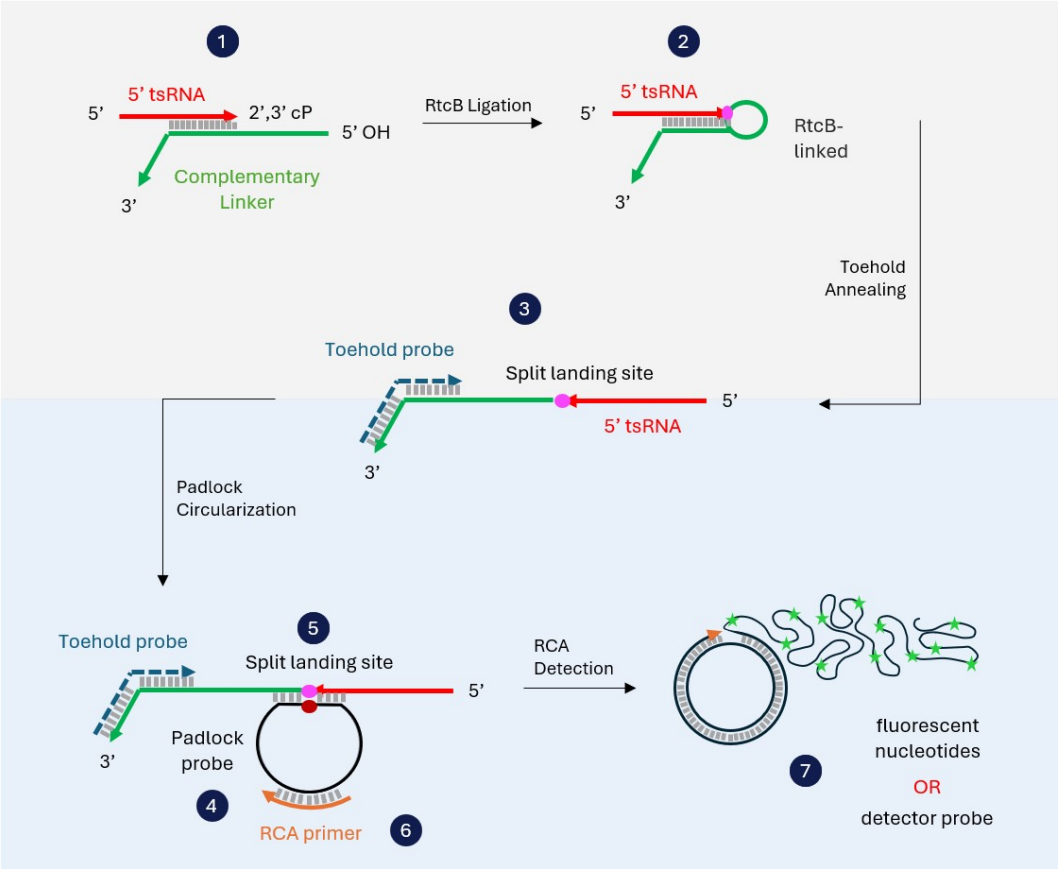

Figure 4.3: Schematic overview of the method development.
(grey) RTCB-mediated ligation and (blue) RCA-based detection for 5' tsRNA-Gly^{GCC} as target.

structure incorporated a split-landing site in closed conformation, which was necessary for padlock probe hybridization.

❸ Padlock Probe Accessibility: To make the ligation-mediated link between specific 5' tsRNA and CL accessible as a platform for signal amplification, an additional 3' terminal sequence on the linker served as a toehold for subsequent padlock probe entry.

❹-❺ Padlock Probe Hybridization and Circularization: The padlock probe hybridized to the split-landing site, which consisted of 18 nucleotides from the 5' tsRNA and 18 nucleotides from the CL. This enabled T4 DNA ligase to circularize the padlock probe, forming a stable closed-loop structure.

❻ RCA Initiation: A DNA primer, complementary to the reporter sequence, initiated RCA, generating long single-stranded DNA amplicons.

❼ Fluorescent Signal Generation: RCA was performed using fluorescently labeled deoxyuridine triphosphate (dUTP), which can be used in place of deoxythymidine triphosphate (dTTP) during amplification to generate densely labeled RCPs.
In an alternative strategy, fluorophore-labeled decorator probes were hybridized to the repetitive sequences within the RCA amplicons to enable visualization.

Various approaches were tried to optimize the different steps. Results are described in greater detail in chapter 5.

4.6.1 RTCB-mediated Ligation

In vitro Protocol

The hybridization process involved mixing 5' tsRNA (AD137) and CL (DK005 or DK008) in water, followed by incubation at 95°C for 3 minutes. Subsequently, RTCB reaction buffer was introduced, and the mixture was gradually cooled to RT in 0.1°C per seconds steps using a thermocycler. Doing this was supposed to linearize RNA and DNA, and ensure optimal conditions for efficient hybridization. $MnCl_2$, GTP, and RTCB ligase were then added in volumes according to Table 4.9, and the reaction mixture was allowed to incubate overnight at 37°C.

Table 4.9: *in vitro* RTCB reaction mix

Reagent	**Volume [µl]**
tsRNA (10 µM)	1
linker (10 µM)	1
10x RTCB buffer	2
5 mM GTP	2
10 mM $MnCl_2$	2
RTCB ligase (24.9 µM)	0.6
Water	11.4
Total	20

Following the ligation reaction, an equal volume of 2x RNA loading dye was added, and the mixture was incubated at 95°C for 3 minutes. The mobility of ligation products was assessed using denaturing urea-PAGE in 0.5x TB buffer,

followed by staining with SYBR-gold and visualization using a GelDoc device (BioRad).

In situ Protocol

Preparation

HeLa cells were cultured in 8-well microscopy chamber slides at a density of 3 $\times$ 10^3 cells/well in DMEM+F/G/P/S for 24 hours at 37°C in a CO_2 incubator. Liposomal transfection using 150 ng of 5' tsRNA-Gly^{GCC} (AD137) was performed overnight. The cells on the slide were washed with 1$\times$ PBS buffer for 5 minutes and fixed (A) with 3% glyoxal in 1 x PBS for 20 minutes on ice for the first experiments and then (B) with 4% PFA in 1$\times$ PBS for 10 minutes at RT. After fixation the cells were washed with 1$\times$ PBS buffer for 5 minutes, and permeabilized with 0.1% Triton-X 100 in 1x PBS for 10 minutes and 0.1 µg/ml proteinase K in 40 mM Tris-HCl (pH 7.4) for 5 minutes. After, post-fixation with 4% PFA for 10 minutes at RT, cells were washed twice with 1x PBS buffer for 5 minutes.

Linker Hybridization

The hybridization reaction in HeLa cells was performed in 100 µl/well of hybridization mixture (1.5 µg oligonucleotide DK005 in 15% FA hybridization solution) overnight at 37°C in a humidified chamber. Afterwards, cells were washed three times with 2x SSC for 10 minutes.

RTCB Ligation

Cells were washed three times with 150 µl 1x RTCB ligation buffer for 10 minutes. Equilibration followed using the pre-ligation buffer mix (Table 4.10) at 37°C for 30 minutes. Subsequently, buffer mix was removed and cells were incubated with RTCB reaction mix (Table 4.10) overnight at 37°C in a humidified chamber. Cells were washed three times with 1x PBS for 5 minutes and once with 2x SSC for 10 minutes.

Toehold Hybridization

Equilibration was performed using 150 µl hybridization buffer for 10 minutes. The hybridization reaction was performed in 100 µl of hybridization mixture (1.5 µg oligonucleotide DK015 in pre-warmed 15% FA hybridization solution) for 3 hours at 37°C, then 1 hour at 50°C, and again 1 hour at 37°C in a humidified chamber.

Table 4.10: *in situ* RTCB pre-ligation and ligation mix

	Pre-ligation buffer mix	**RTCB reaction mix**
Reagent	**Volume [µl]**	
10x RTCB reaction buffer	20	10
$MnCl_2$ (10 mM)	20	10
GTP (10 mM)	10	5
RTCB ligase (24.9 µM)		3
Water	150	72
Total	200	100

4.6.2 RCA-based Detection

In vitro Protocol

Probe Immobilization on Paramagnetic Beads

First, as a preparation 40 µg of streptavidin-coated paramagnetic beads were washed three times with 500 µl of 1× TE buffer using a permanent magnet. The RTCB reaction mixture of template 5' tsRNA-Gly^{GCC} and 3' biotinylated linker (DK008) supplemented with 15% formamide together with 100 pmol toehold probe (DK015) was heated to 95°C and slowly cooled to RT to allow formation of a double stranded complex. Biotinylated probes were immobilized on the beads for 30 minutes and then washed three times with 1x TE to remove any unbound probes.
As a control for the RCA reaction, another DNA oligonucleotide (DK014), which is identical to the target sequence within the ligation product at the split-landing site, was utilized.

Padlock Circularization on Immobilized Probes

Beads with immobilized probes were prepared by suspending them in 100 µl of 1× CutSmart buffer containing 100 pmol padlock probe DK009. The padlock probe was first denatured at 95°C for 3 minutes and snap-cooled on ice before the addition of CutSmart buffer. The beads were incubated with the padlock mixture at 37°C for 30 minutes, followed by two washes with 1× CutSmart Buffer. For padlock circularization, the beads were equilibrated in 1× T4 DNA ligase buffer for 10 minutes, after which 0.5 µl of T4 DNA ligase was added.

The ligation reaction was carried out at 37°C for 60 minutes. Following ligation, the beads were washed three times with 1× TE buffer to remove unligated components.

RCA Reaction on Immobilized Probes

To initiate RCA, 100 µl of 1x CutSmart buffer containing 100 pmol of the denatured RCA primer DK018N was added to the beads. After a 30-minute incubation at 37°C, the beads were washed twice with 1× CutSmart buffer and equilibrated in 1× Φ29 DNA Polymerase buffer for 10 minutes. The reaction mixture was prepared in 60 µl of extension buffer according to Table 4.11. The extension reaction was carried out at 37°C for 1 hour or overnight with continuous mixing.

Table 4.11: *in vitro* Φ29 DNA Polymerase-amplification mix

	labeled dUTP mix	**unlabeled mix**
Reagent	**Volume [µl]**	
10x Φ29 Polymerase buffer	6	6
dNTPs (10 mM)	1	1
aminoallyl-dUTP (1 mM)	1	
BSA (20 mg/ml)	0.5	0.5
Φ29 DNA Polymerase (10 µM)	1	1
Water	42.5	43.5
Total	60	60

After the RCA reaction, the beads were incubated in 60 µl 100% FA at 95°C for 5 minutes to disrupt the streptavidin/biotin interaction and release the RCA amplicons into solution. A quarter volume of 6× DNA loading dye was added to the mixture, followed by an additional incubation at 95°C for 3 minutes to ensure complete denaturation. The RCA products were analyzed by 0.5% agarose gel electrophoresis in 1× TAE buffer, and visualization was performed using a GelDoc imaging system or by subsequent Southern blotting.

In situ Protocol

Preparation

HeLa cells were prepared in 8-well microscopy chamber slides at a density of 3 × 10^3 cells/well as described in section 4.6.1. Liposomal transfection using 150

ng of the DNA oligonucleotide DK019 was performed as a control for testing the RCA reaction *in situ*.

Padlock Hybridization

The hybridization reaction was performed in 100 µl of hybridization mixture (1.5 µg padlock probe DK009 in 15% FA hybridization solution) for 5 hours or overnight at 37°C in a humidified chamber. Cells were washed three times with PBS-T for 10 minutes and once with 1x PBS for 5 minutes.

Padlock Circularization

The ligation of padlock probes was performed with 30 U of T4 DNA ligase in 100 µl of 1× T4 DNA ligase buffer for 1 hour at 37°C in a humidified chamber. Afterwards, cells were washed three times with 1x PBS for 5 minutes.

RCA Initiation

The primer hybridization was performed in 100 µl of hybridization mixture (1.5 µg oligonucleotide DK018N in hybridization solution containing 2x SSC, 20% FA) for 30 minutes at 37°C in a humidified chamber. Cells were washed three times with 1x PBS for 5 minutes. The RCA was performed with 30 U of Φ29 DNA polymerase in 100 µl of according Φ29 DNA polymerase amplification mix (Table 4.12) for 1 hour or overnight at 37°C in a humidified chamber. Afterwards, cells were washed three times with 1x PBS for 5 minutes.

RCA Detection

If RCA products were not detected using labeled nucleotides, they were visualized through hybridization with fluorescently labeled oligonucleotides (DK012N). Hybridization was performed in 100 µl of hybridization mixture (1.5 µg DK012N in 2x SSC, 20% FA) for 30 minutes at 37°C in a humidified chamber. Following hybridization, the glass slide was washed three times with 1x PBS for 10 minutes each. The samples were then post-fixed with 4% PFA for 10 minutes at RT, followed by two additional 5-minute washes with 1x PBS.

After washing, cells were incubated with Hoechst (1 µg/ml) in 1x PBS for 10 minutes at RT, followed by a final 10-minute wash in 1x PBS. Coverslips were then briefly dipped in distilled water, gently tapped onto a paper towel to remove excess liquid, and mounted onto a glass slide with a drop of mounting medium.

Table 4.12: *in situ* Φ29 DNA Polymerase-amplification mix

	labeled dUTP mix	**detector probe mix**
Reagent	**Volume [µl]**	
10x Φ29 Polymerase buffer	10	10
dNTPs (10 mM)	1	1
aminoallyl-dUTP (0.2 mM)	1	
BSA (20 mg/ml)	0.5	0.5
Φ29 DNA Polymerase (10 µM)	1	1
Water	86.5	87.5
Total	100	100

4.7 Computational Methods

Fluorescence Image Aquisition and Analysis

Cell were observed on the slides by laser scanning microscopy using an Olympus FV3000 confocal microscope. Excitation laser sources and emission ranges were 405 nm/400-510 nm (DAPI, shown as blue), 488 nm/510-560 nm (Atto 488, shown as green), and 565 nm or 590 nm/560-700 nm (Atto 565 or Atto 590, shown as red). All images were processed using ImageJ.

5 Results

The foundational steps for establishing the detection methodology for a specific 5' tsRNA were first conducted under controlled *in vitro* conditions. By systematically testing and optimizing reaction parameters, such as enzyme concentrations, reaction times, and hybridization conditions, the efficacy of both processes - RTCB-mediated ligation and RCA-mediated detection - was assessed. These experiments served as the basis for validating key steps in the detection strategy, ensuring reproducibility and reliability before advancing to establishing the methodology *in situ*.

5.1 RTCB-mediated Ligation of Ectopic 5' tsRNAs *in vitro*

RTCB ligation activity was assessed *in vitro* using urea-PAGE with SYBR gold staining to evaluate its ability to covalently join synthetic 5' tsRNAs to a complementary linker (CL). The ligation product was identified by its size and an upshift in electrophoretic mobility, reflecting the combined lengths of the tsRNA and CL.

Initial tests confirmed successful ligation of 5' tsRNAs to a fully complementary linker MattVIE426. To refine the methodology, ligation efficiency was further tested using partially complementary linkers with varying hybridization region lengths. Among the designs tested, DK005 showed the highest ligation efficiency, visible as intense signals at 90 nt (Figure 5.1), and was therefore selected for further method development. Unligated probes were visible as signals of the same molecular size as the input. There were no indications that ligation was influenced by increasing linker concentration.

To confirm the identity of the ligation product, nucleic acids were extracted following *in vitro* RTCB ligation reactions and gel purification. RT-PCR was performed using a primer specific to the CL end. SYBR gold staining revealed a predominant PCR product corresponding to the expected size of 50 bp (Fig-

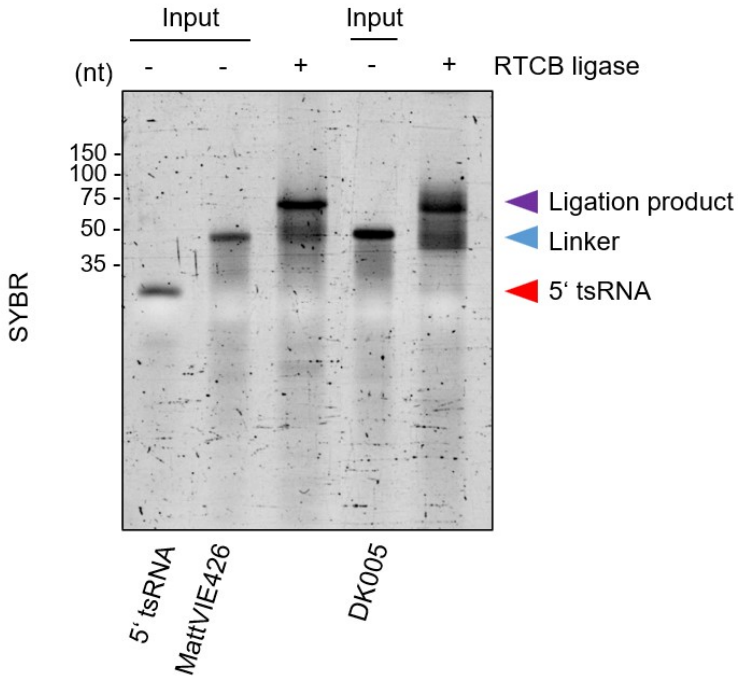

Figure 5.1: Test of RTCB-mediated ligation *in vitro*.
10 pmol of synthetic 5' tsRNA (AD137) was hybridized to 10 pmol of a complementary linker oligonucleotide (MattVIE426 or DK005) and afterwards ligated by RTCB ligase. The ligation efficiency was assessed on a 15% denaturing urea-PAGE with SYBR gold staining. Successful ligation of both components resulted in a higher molecular weight product, evident as an upward shift in band migration.

ure 5.2), confirming that RTCB successfully ligated the 5' tsRNA containing a cycP to the linker oligonucleotide. The sequence identity of the ligation product was further validated through Sanger sequencing. Sequence analysis of cloned RTCB ligation products revealed that the ligated RNA/DNA products not only contained the sequence expected but also shortened sequences with missing nucleotides at the ligation site. This was particularly the case, when TOPO cloning was performed directly upon ligation reaction without prior gel purification of the ligation product. Here, a sequence truncation of 16 nucleotides on the RNA 3' end was detected.

For economic reasons, recombinant RTCB was expressed and purified in house and its ligation efficiency was compared to commercial RTCB in ligation reactions of synthetic 5' tsRNA and DK005. SYBR staining showed that recombinantly expressed RTCB (1.125 mg/ml) showed enhanced ligation efficiency when compared to the same concentration of RTCB purchased from NEB (data not shown).

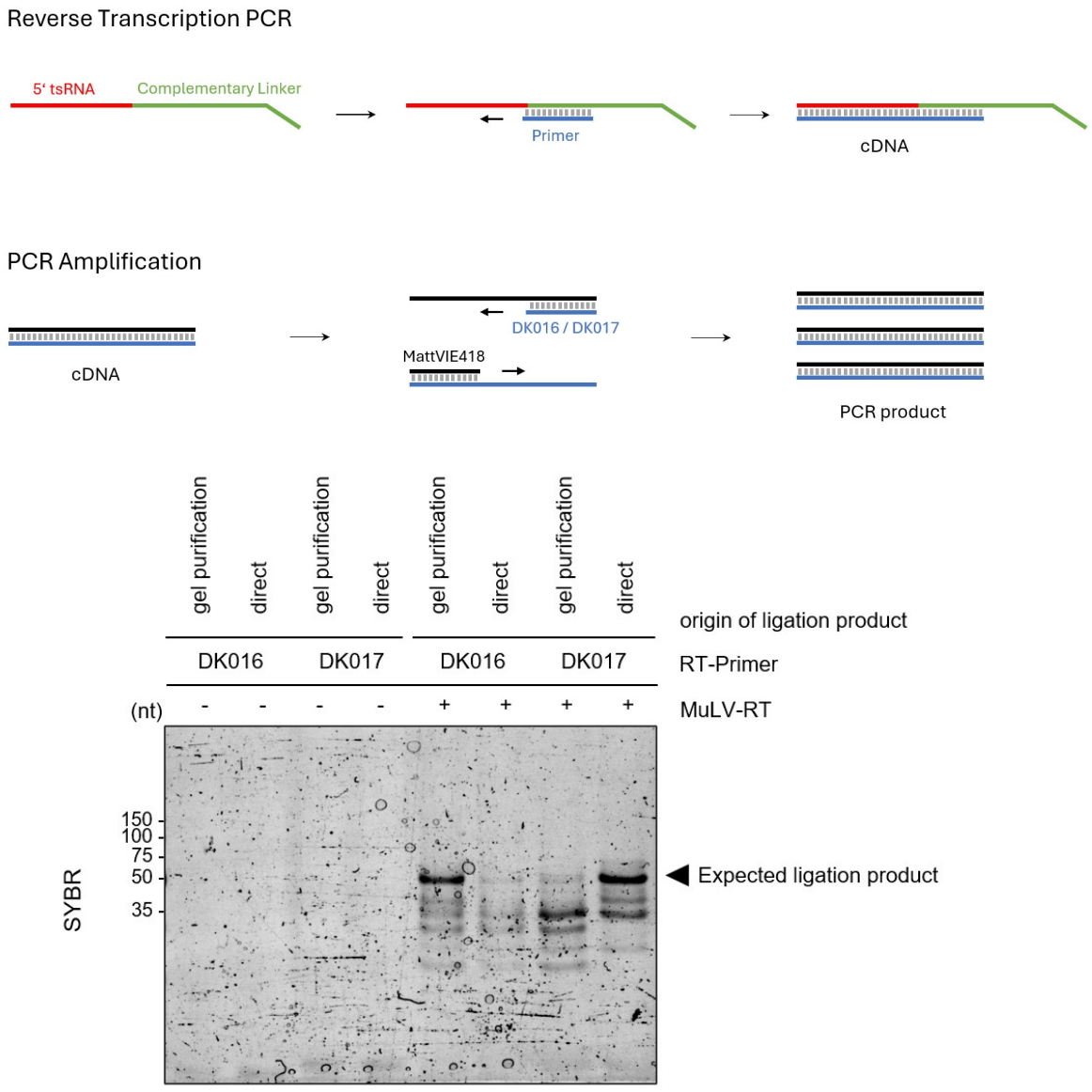

Figure 5.2: Validation of *in vitro* ligation by RT-PCR.
RTCB ligation product from synthetic 5' tsRNA (AD137) and linker (DK005) was extracted from a 15% denaturing urea-PAGE or used directly upon RTCB-mediated reaction for first strand cDNA synthesis by M-MuLV RT followed by PCR amplification. The PCR product was tested on an 8% non-denaturing polyacrylamide gel and SYBR gold stained.

5.1.1 Optimization of Ligation Time

To evaluate the impact of ligation time on RTCB-mediated ligation *in vitro*, reactions were once again analyzed using denaturing urea-PAGE. Specifically, the ligation efficiency was assessed by varying the incubation time while keeping the concentration of substrates constant. The results revealed that increasing the ligation time improved efficiency up to a plateau at 6 hours, beyond which no further increase in ligation products was observed. Shorter incubation times

resulted in incomplete ligation, which was shown by a lower yield of ligated products and the presence of unreacted substrates.

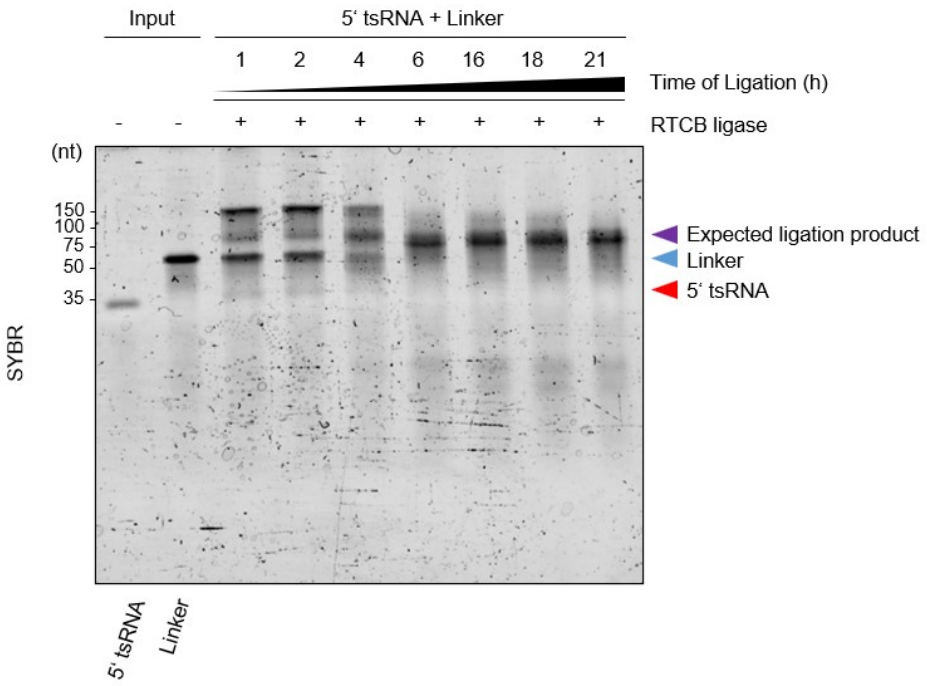

Figure 5.3: Comparison of ligation efficiency using different ligation times. 10 pmol of synthetic 5’ tsRNA (AD137) was hybridized and ligated to 10 pmol of complementary linker (DK005) using homemade RTCB ligase. Ligation efficiency was tested after indicated time points and analyzed using a denaturing 15% polyacrylamide gel and SYBR gold staining.

At shorter ligation times, high-molecular-weight polymers were observed above the expected ligation product size. However, later experiments showed similar polymer formation also in overnight ligation reactions. Despite their presence, these polymers did not interfere with subsequent RCA amplification, suggesting that they likely dissociate during downstream steps involving higher stringency buffers.

5.1.2 Optimization of RTCB Concentration

Following the evaluation of ligation time, the impact of RTCB concentration on ligation efficiency was analyzed to further optimize the reaction conditions. Reactions were performed with varying RTCB concentrations while keeping the substrate levels constant.

The results revealed that increasing RTCB concentration did not necessarily lead to enhanced ligation efficiency. However, a maximum yield of ligated products was observed at the highest concentration tested, which was decided to be the optimal enzyme concentration.

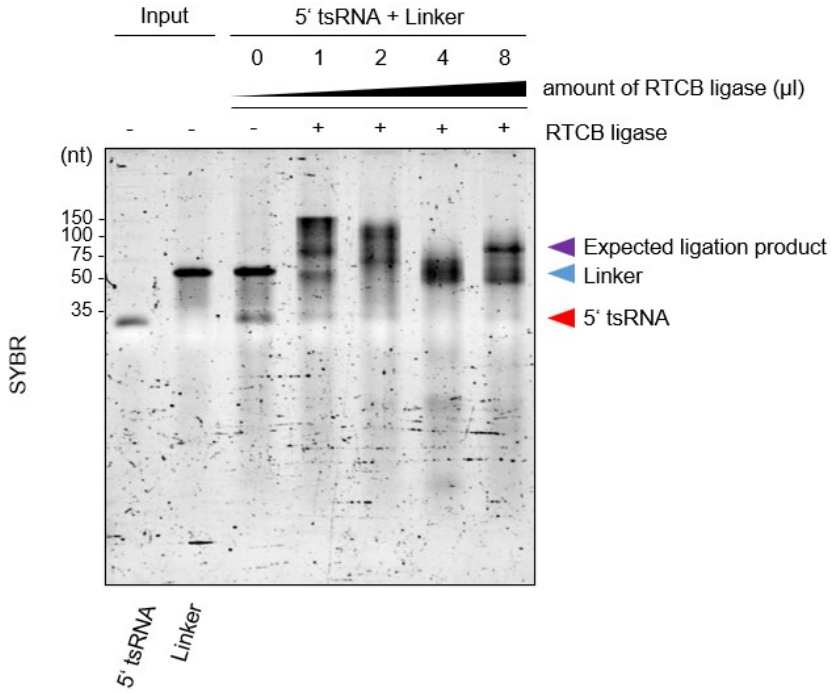

Figure 5.4: Comparison of ligation efficiency using different RTCB concentrations.
10 pmol of synthetic 5' tsRNA (AD137) was hybridized and ligated to 10 pmol of complementary linker (DK005). Ligation efficiency using 0, 2, 4, 6, and 8 µl of RTCB were tested and analyzed using a denaturing 15% polyacrylamide gel and SYBR gold staining.

5.1.3 Optimization of Cofactor Concentration

To investigate the lack of complete ligation efficiency, the impact of increasing the final GTP concentration was tested. It was hypothesized that GTP might be a limiting factor in RTCB-mediated ligation. This hypothesis was based on a study by Popow *et al.*, who demonstrated enhanced RTCB ligase activity with elevated GTP levels [41].

As shown in Figure 5.5, increasing the GTP concentration from 0.1 mM (lanes 3-6) to 0.5 mM (lanes 7-10) significantly stimulated RTCB ligase activity, supporting the assumption that optimal GTP levels are important for efficient ligation.

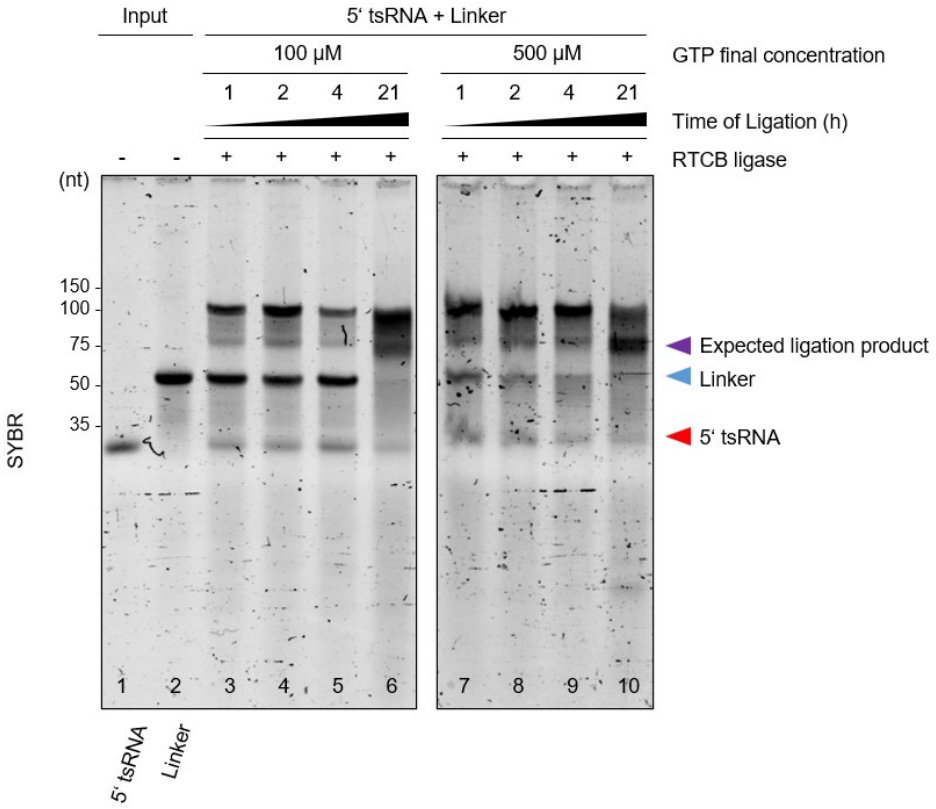

Figure 5.5: Ligation efficiency is depending on GTP concentration.
5 pmol of synthetic 5’ tsRNA (AD137) was hybridized and RTCB-ligated to 5 pmol of complementary linker (DK005). Different concentrations of the cofactor GTP were included into the RTCB-mediated ligation. RTCB-ligation products were analyzed using a denaturing 15% polyacrylamide gel and SYBR gold staining.

5.1.4 Testing the Influence of Archease

In the previous section, it was demonstrated that longer ligation times enhance RTCB-mediated ligation efficiency *in vitro*. To further explore this, the potential effect of archease on ligation efficiency was assessed *in vitro* in combination with varying ligation times. Archease has previously been shown to interact with RTCB or its substrates to accelerate ligation efficiency [42].

Figure 5.6 indicates that while archease may facilitate faster ligation during shorter incubation periods (lanes 5-7), it does not enhance overall ligation efficiency over prolonged reaction times. Notably, the ligation product in lane 4 (21 hours without archease) shows a more intense band compared to lane 8 (21 hours with archease), suggesting that archease does not surpass the efficiency achieved by extended incubation in the absence of archease.

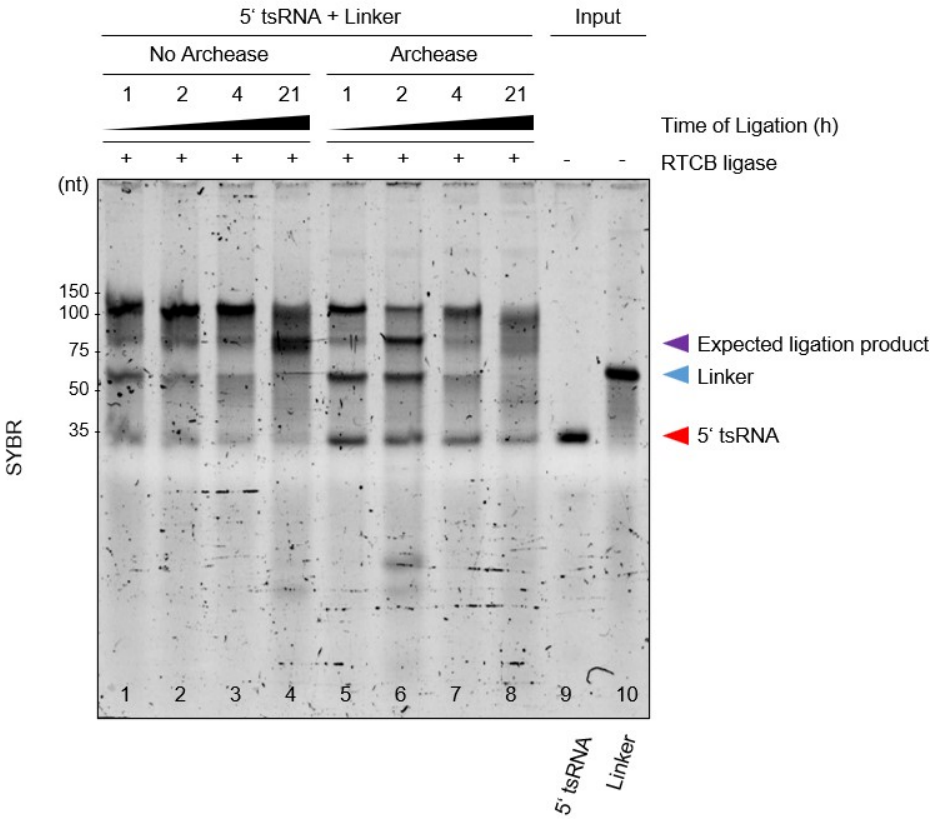

Figure 5.6: Archease does not enhance RTCB-mediated ligation efficiency using longer ligation times.
5 pmol of synthetic 5' tsRNA (AD137) was hybridized and RTCB-ligated to 5 pmol of complementary linker (DK005) in the absence or presence of archease. Ligation reactions were performed for the indicated ligation times and analyzed using a denaturing 15% polyacrylamide gel and SYBR gold staining.

5.1.5 Testing the Influence of PEG 8000

PEG 8000 was tested for its potential to improve reaction efficiency in RTCB-mediated ligation. According to the manufacturer's instructions, the inclusion of 15% (w/v) PEG 8000 is known to significantly stimulate ligation activity, likely by promoting macromolecular crowding to bring enzymes in closer proximity to their substrates. However, tests indicated no change in ligation efficiency under the tested conditions (data not shown).

5.2 RCA-based Detection of RTCB-ligated Platform (R-LP) *in vitro*

In the previous chapter, it was demonstrated that RTCB ligase activity can be utilized to create a target sequence suitable for rolling circle amplification

(RCA). This sequence will henceforth be referred to as the **RTCB-ligated platform** (R-LP).

To test and optimize the RCA protocol *in vitro*, a surface-immobilized format was employed. Streptavidin-coated magnetic beads were used as the solid support in these experiments due to their ability to retain the biotinylated platform during washing steps, buffer exchanges, and even under stringent conditions.

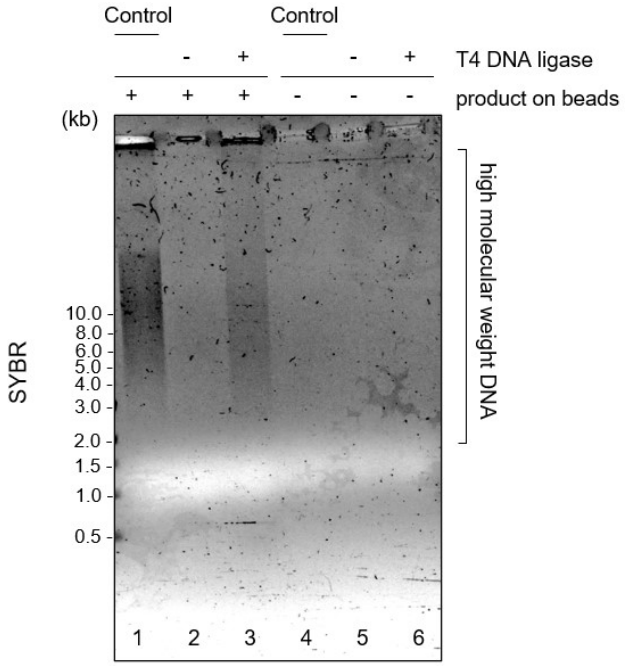

Figure 5.7: Detection of 5′ tsRNA-Gly^{GCC} *in vitro* based on RCA.
RTCB ligation product from 10 pmol 5′ tsRNA (AD137) and 10 pmol biotinylated linker (DK008) was used directly upon RTCB-mediated reaction. RCA reaction was performed on R-LP bound to 4 µl streptavidin-coated beads. Control RCA reactions were performed using 10 pmol of a sequence mimicking the R-LP (DK014). RCA reaction products were analyzed by electrophoresis through 0.5% agarose gel and SYBR green staining before and after release from beads.

Amplification activity was assessed *in vitro* on agarose gels stained with SYBR green. Gel analysis of RCA products revealed high molecular weight DNA, visible as a diffuse signal significantly longer than the ligated platform immobilized on the beads (lanes 1 and 3, Figure 5.7). This confirmed that the observed DNA was the product of continuous strand displacement synthesis catalyzed by Φ29 polymerase.

Initially, a biotinylated oligonucleotide mimicking the RTCB-ligated platform

(DK014) was tested as a control (lane 1, Figure 5.7). Subsequently, 5' tsRNA was ligated via its 3' cycP moiety to a biotin-labeled CL (DK008), forming the R-LP (lane 3, Figure 5.7). For all RCA experiments, a specific padlock probe (DK009) was used, designed with 5' and 3' ends complementary to the hybridization region of the ligated platform.

The specificity of RCA-mediated detection was confirmed through a series of control experiments. No amplification was detected in reactions lacking T4 DNA ligase (lane 2, Figure 5.7), indicating that RCA products originated exclusively from ligated and circularized padlock probes. Likewise, amplification was absent in reactions in which the R-LP had not been generated prior by omitting the RTCB ligase during RTCB-mediated ligation.

5.2.1 Testing the Toehold Probe

To enhance RCA efficiency, it was hypothesized that making the R-LP accessible for the padlock probe is a critical step for successful amplification. While it was expected that the structure might partially "open" on its own due to equilibrium dynamics, the introduction of a toehold probe was anticipated to facilitate this process more effectively. A toehold probe (DK015) was specifically designed to hybridize with the 3' end of the linker, targeting the junction region between the 5' tsRNA and CL. By binding within this region, the toehold probe was expected to disrupt secondary structures, thereby "opening" the ligation product. This structural disruption would expose the split-landing site of the R-LP and enhance its accessibility for hybridization with the padlock probe, thereby ultimately enabling more efficient RCA amplification (Figure 4.3).

To further confirm the identity of the RCA products, an oligonucleotide probe (DK018), complementary to the RCA primer, was designed and radiolabeled for use in Southern blotting experiments. As shown in Figure 5.8, the Southern blot confirmed the heterogeneous nature of the amplified DNA sequence, which is characteristic of repetitive RCA products. Additionally, the Southern blot revealed enhanced RCA efficiency when a toehold probe was incorporated into the protocol, as indicated by significantly stronger signals in lane 3 (with toehold probe) compared to lane 2 (without toehold probe) in Figure 5.8.

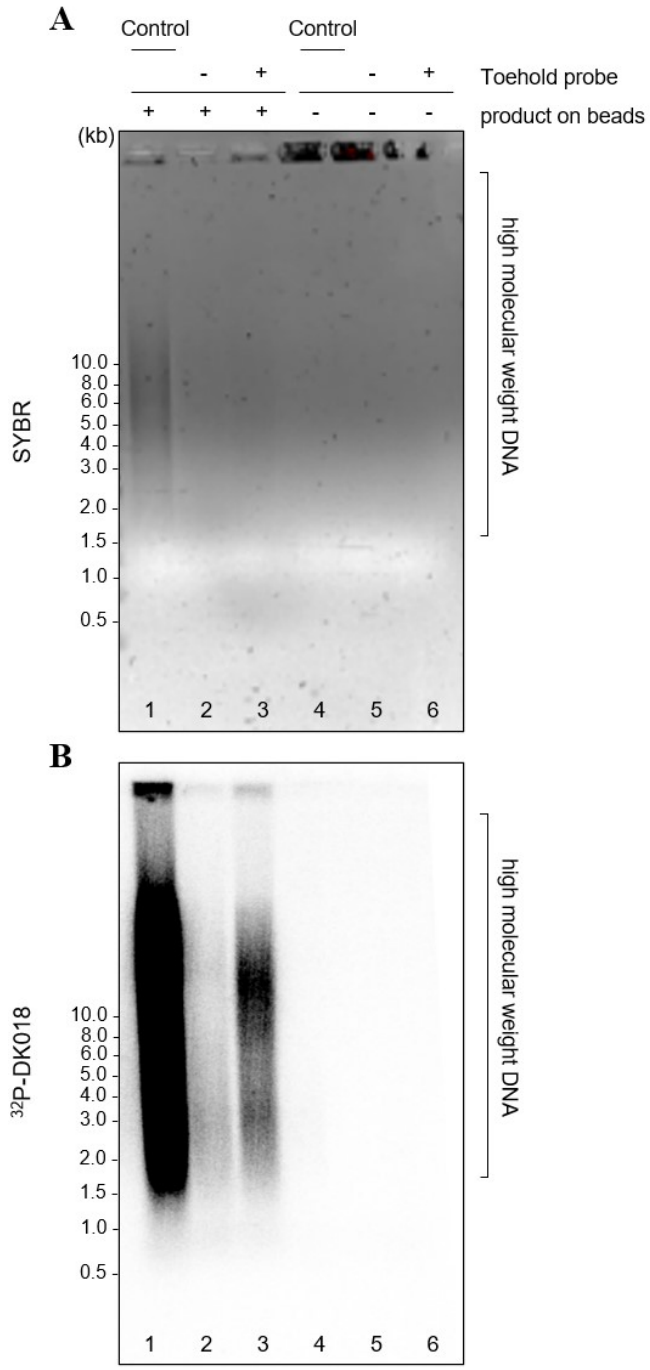

Figure 5.8: Toehold probe increases efficiency of RCA-based detection. Reactions were carried out under the conditions described in Materials and Methods. (**A**) RTCB ligation product from 10 pmol 5' tsRNA (AD137) and 10 pmol linker (DK008) was used directly upon RTCB-mediated reaction. RTCB reaction mixture was combined with 1.5 µM of toehold probe. After denaturation, temperature of the mixture was ramped down to 71°C, to enable toehold probe annealing prior to RCA-based detection. Control RCA reactions were performed using 10 pmol of a sequence mimicking the R-LP (DK014). RCA reaction products were analyzed by electrophoresis through 0.5% agarose gel and SYBR green staining before and after release from beads. (**B**) Specific RCA products were detected using southern blotting and hybridization to a radioactively-labeled probe (DK018) complementary to the detector sequence.

5.2.2 Testing Incorporation of Fluorescent Nucleotides

To prepare for *in situ* applications, the detection of RCA products was tested using fluorescently labeled dUTPs. Incorporating these labeled nucleotides into the repetitive RCA sequence allowed direct visualization under UV light, eliminating the need for SYBR green staining. The level of amplification observed was directly influenced by the amount of fluorescently labeled nucleotides incorporated into the RCA extension product.

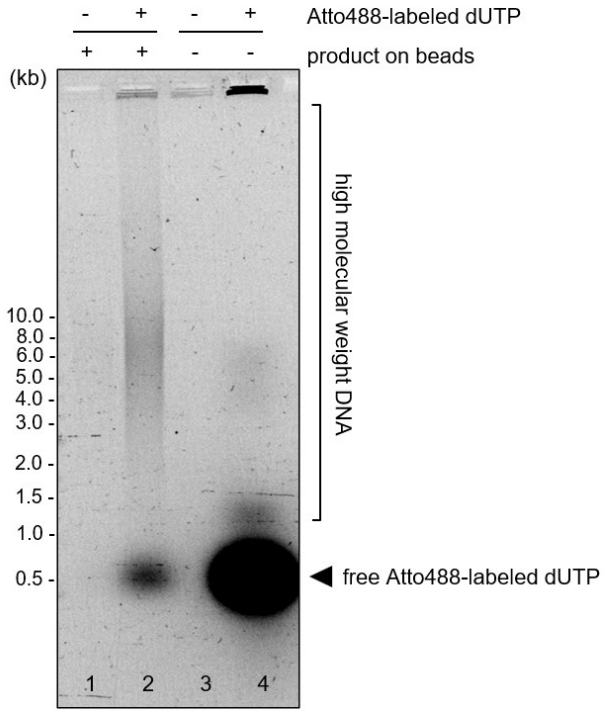

Figure 5.9: Detection of RTCB-ligation products *in vitro* using fluorescently labeled dUTP.
RTCB ligation product from 10 pmol 5' tsRNA (AD137) and 10 pmol linker (DK008) was used directly upon RTCB-mediated reaction. RTCB reaction mixture was combined with 1.5 µM of toehold probe. After denaturation, temperature of the mixture was ramped down to 71°C, to enable toehold probe annealing prior to RCA-based detection with dTTP substitution by (10%) Atto488-dUTP. RCA reaction products were analyzed by electrophoresis through 0.5% agarose gel and SYBR green staining before and after release from beads.

Initial experiments focused on determining the optimal concentration of labeled dUTP to balance visibility and polymerase efficiency. Sufficient incorporation was necessary to produce detectable RCA products, while excessive concentrations of fluorescent nucleotides inhibited polymerase activity. A ratio of 1:10 Atto488-labeled dUTP to unlabeled dTTP was identified as optimal, providing strong fluorescence signals without compromising RCA efficiency.

The strong fluorescent signal near 500 bp is due to the fluorophore of the free dUTP, which migrates at this position in the native gel.

5.2.3 Testing the Influence of Formamide

The impact of different formamide concentrations on the hybridization efficiency of the toehold probe was carefully tested to find the best conditions as prerequisite for RCA. As previously mentioned, formamide is a denaturant that destabilizes non-covalent bonds, thereby disrupting secondary structures. By doing so, formamide makes it easier for probes to bind to their targets *in vitro* as well as *in situ* [43].

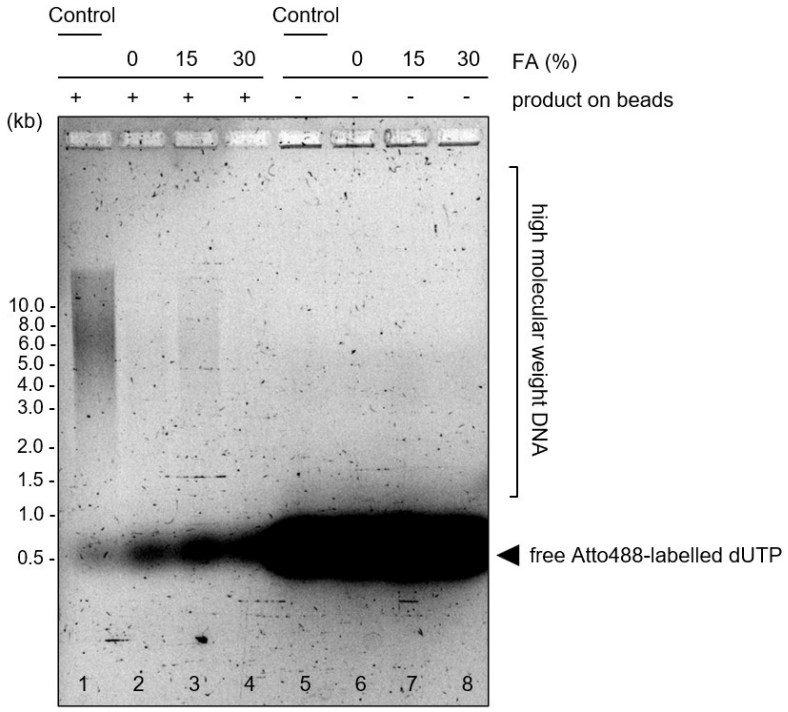

Figure 5.10: Moderate formamide concentration impacts toehold probe annealing.
RTCB ligation product from 10 pmol 5' tsRNA (AD137) and 10 pmol linker (DK008) was used directly upon RTCB-mediated reaction using homemade RTCB ligase. RTCB reaction mixture was combined with 1.5 µM of toehold probe in the presence of either 0, 15, or 30% (w/v) formamide. After denaturation, temperature of the mixture was ramped down to 71°C, to enable toehold probe annealing prior to RCA-based detection. Control RCA reactions were performed using 10 pmol of a sequence mimicking the R-LP (DK014). RCA reaction products were analyzed by electrophoresis through 0.5% agarose gel and SYBR green staining before and after release from beads.

The results showed that moderate concentrations (15% w/v) of formamide produced the strongest RCA fluorescence signal as seen in lane 3 of Figure 5.10.

When no formamide was used, secondary structures of ligated products were not fully disrupted, leading to weaker signals. On the other hand, at higher formamide concentrations (30% w/v), probe binding efficiency is diminished relative to that at 0% (w/v) formamide, likely because the probe-target duplex becomes unstable.

5.3 Specific RCA-based Detection of Transfected R-LP in Fixed HeLa cells

From previous chapters, it became clear that development of the RCA-based assay necessitates an efficient RTCB-mediated ligation of 5' tsRNAs to be able to construct the R-LP in high and constant concentration. To circumvent this limitation and to be able to test the RCA approach without fluctuating concentration of the initiating platform, the use of an oligonucleotide (DK019) mimicking the split-landing site of the R-LP to proceed with the protocol's optimization was necessary. This probe was utilized to provide a stable and reproducible substrate for testing, as it bypassed the dependency on RTCB-mediated ligation in the initial optimization steps. Therefore systematic testing of downstream processes - such as padlock hybridization, T4 DNA ligation, and signal detection - was possible without the variability introduced by incomplete ligation.

5.3.1 Assessment of Fixation Parameters

Selecting the right fixative is essential to preserve cellular and nuclear structures while maintaining target nucleic acid accessibility for hybridization. Proper structural preservation ensures efficient and accurate probe binding, with the addition of formamide further enhancing binding by denaturing secondary structures.

Among the tested fixatives, 4% PFA provided superior preservation of cellular and nuclear structures after incubation with the chosen hybridization buffer, making it the optimal choice for padlock probe hybridization.

In contrast, early RCA experiments using 3% glyoxal as the fixative resulted in more diffuse transfection and RCA signals compared to 4 % PFA. As a result, RCA signals were distributed throughout the cell rather than being localized primarily in the cytoplasm, as expected.

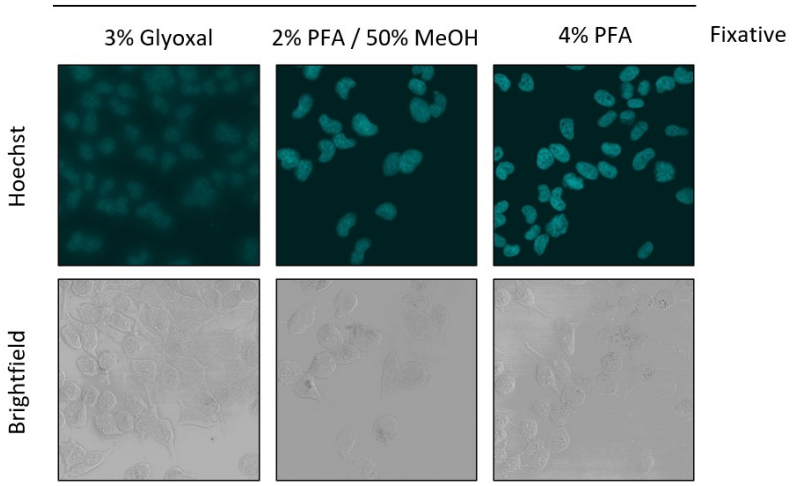

Figure 5.11: Nuclei morphology changes with padlock-hybridization conditions post-fixation with various fixatives.
HeLa cells were fixed with either 3% glyoxal, 2% PFA/50% MeOH, or 4% PFA and incubated in 15% FA Hybridization buffer for 24 hours. Nuclei were stained using Hoechst (blue) and analysis of cell morphology by confocal microscopy followed.

5.3.2 Optimization of Hybridization Buffer

To evaluate the impact on hybridization efficiency, three different hybridization buffer compositions (10%, 15%, and 30% FA hybridization solution) were tested. The formulations were prepared according to established protocols described in Krzywkowski T., *et al.* [44] and Lin C., *et al.* [39]. Particular focus was placed on the hybridization of the padlock probe, as its successful binding was identified as the most critical step in the RCA protocol.

The hybridization efficiency was evaluated *in situ* using a padlock probe labeled with a fluorescent dye conjugated to thymine (T) within its sequence. Using fluorescence microscopy, the padlock probes appeared as distinct green foci. When co-localized with the synthetic platform oligonucleotide labeled with Atto565 (red) - which mimics the RTCB-ligated structure - yellow signals were observed, confirming successful hybridization of the padlock probe *in situ*.

Comparison showed that 10% and 15% FA hybridization solutions generated strong and more specific fluorescence signals with minimal background noise, while the 20% FA hybridization solution led to high accumulation of the padlock probe within the nuclei of cells.

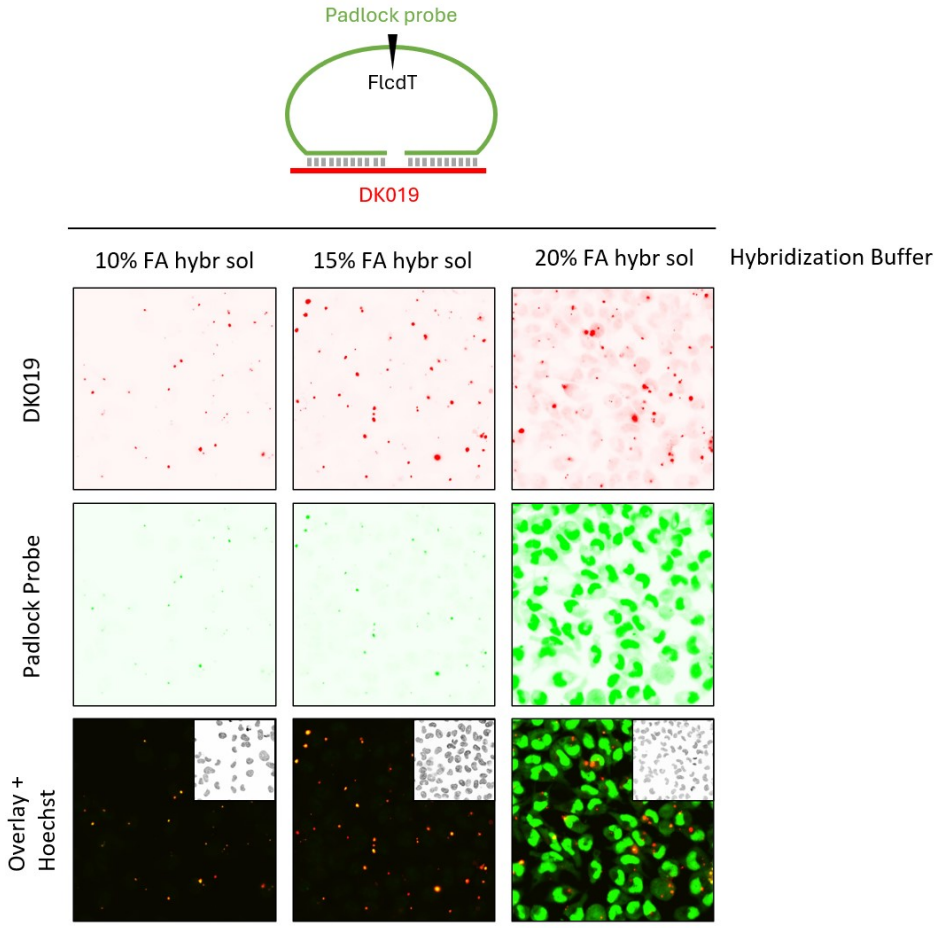

Figure 5.12: Presence of background signal dependent on padlock hybridization buffer.
150 ng of Atto565 (red)-labeled mimic of RTCB-ligated product (DK019) were liposomally transfected into HeLa cells. The cells were fixed using 4% PFA and Fluorescein (green)-labeled padlock probe (DK020) hybridization was performed. Analysis for localization of the transfected oligonucleotide and hybridized probe by confocal microscopy followed.

In the *in situ* RCA protocol, both the fluorescence intensity of RCA signals and background signal directly correlated with the hybridization conditions. 15% FA hybridization solution consistently produced RCA signals that co-localized with the transfected platform, confirming the specificity of signal amplification while maintaining the lowest background noise. In contrast, 10% FA hybridization solution occasionally exhibited variability in signal distribution, likely due to subtle differences in probe binding efficiency. Further experiments tested the effects of incubation time on hybridization efficiency using 15% FA hybridization solution. Similar results were obtained with 5 hours and 24 hours of incubation at 37°C (data not shown).

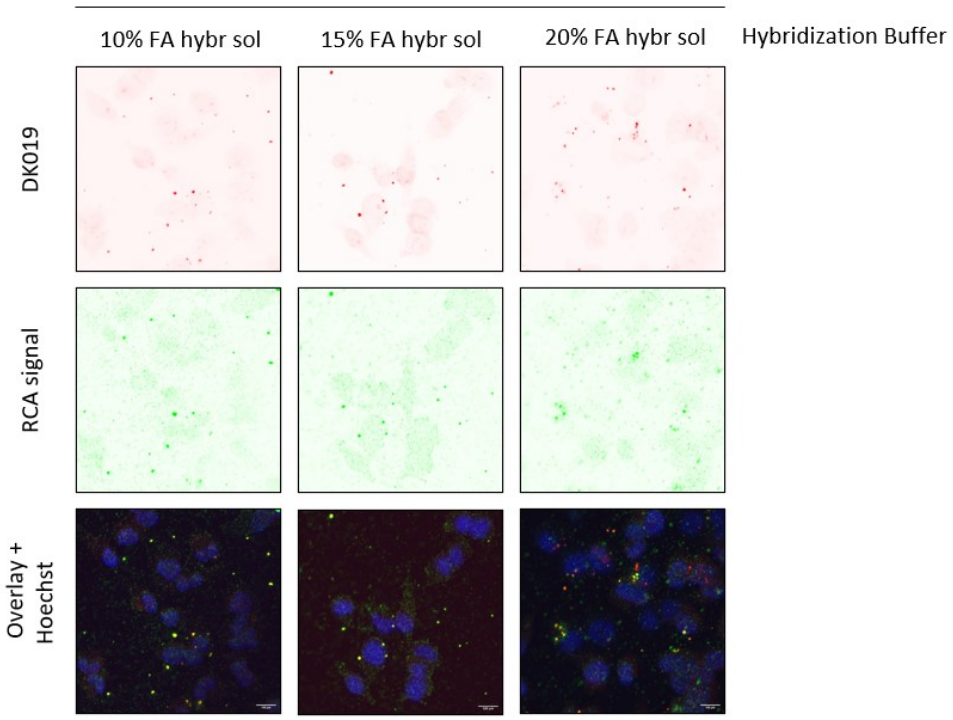

Figure 5.13: Padlock Hybridization buffer influences Background Signal during RCA product detection *in situ*.
150 ng of Atto565 (red)-labeled mimic of RTCB-ligated product were liposomally transfected into HeLa cells using lipofectamine transfection reagent. The cells were kept in transfection media for 24 hours at 37°C, then fixed using 3% glyoxal prior to RCA-based detection. RCA reaction using fluorophore-labeled nucleotides (green) was performed for 24 hours. Analysis for localization of the transfected product and the generated RCA signal by confocal microscopy followed.

5.3.3 Assessment of Detection Method

To detect RCA amplification, initial experiments incorporated fluorescently labeled dUTPs into the DNA during synthesis. As an alternative detection method, subsequent experiments utilized fluorescently labeled detector probes specifically designed to hybridize with RCA products, resulting in more targeted and brighter fluorescence signals (Figure 5.14).

The specificity of RCA-mediated detection was validated by first testing reactions in the absence of T4 DNA ligase. No detectable signal in the green channel confirmed that RCA products in cells exclusively originated from ligated and circularized padlock probes (lane 2, Figure 5.14). Similarly, no amplification was observed when either DK019 (lane 1, Figure 5.14) or the padlock probe (data not shown) was omitted from the reaction.

While the results demonstrated successful RCA amplification from the synthetic platform, the next critical step to test was to achieve similar outcomes with products directly derived from RTCB-mediated ligation.

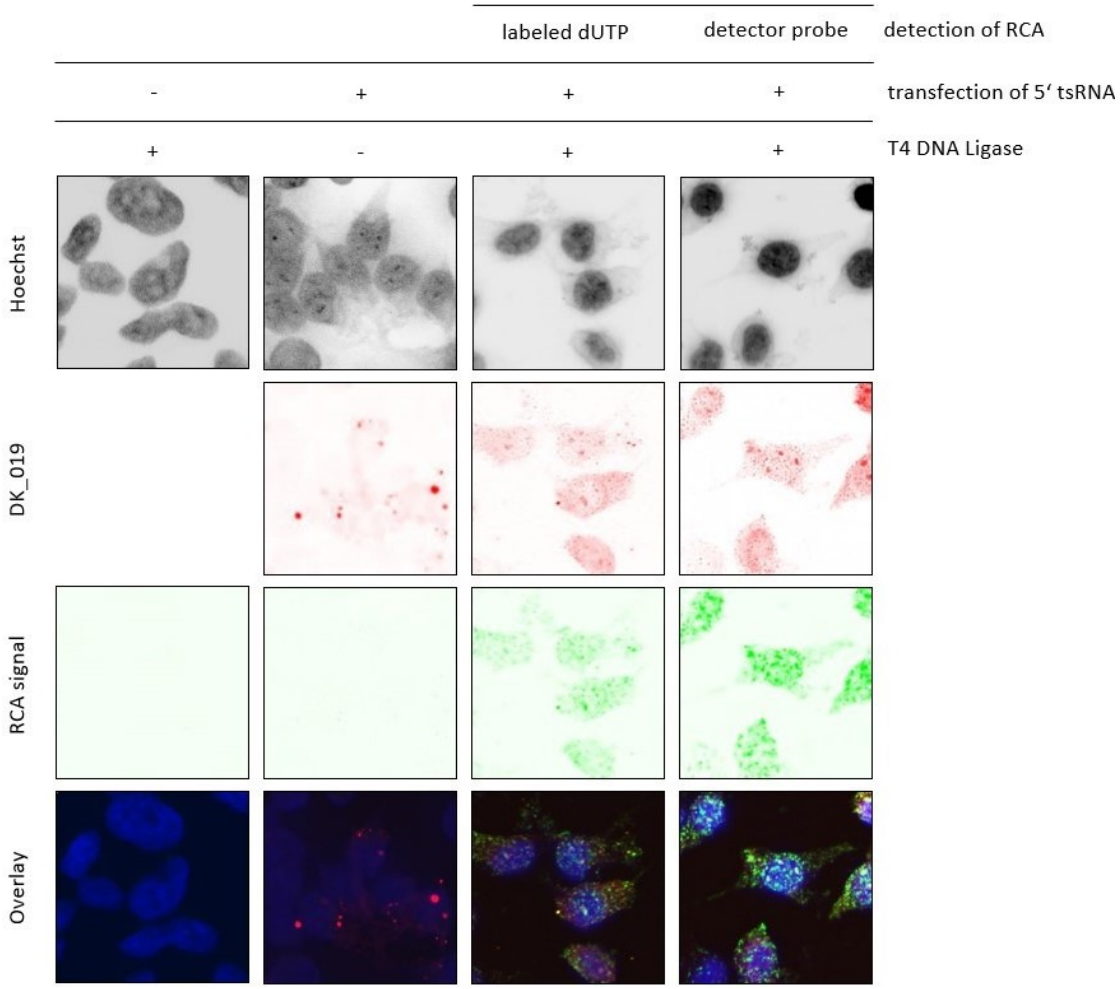

Figure 5.14: Detection of RCA products *in situ*.
Liposomal transfection into HeLa cells was conducted using 150 ng of Atto565 (red)-labeled mimic of RTCB-ligated product (DK019). Afterwards cells were fixed using 3% glyoxal and RCA-based detection was performed. RCA reaction using fluorophore-labeled nucleotides (green) was performed for 5 hours. Analysis for localization of the transfected oligonucleotide and the generated RCA signal by confocal microscopy followed.

5.4 Testing RTCB-mediated Ligation of Ectopically Introduced 5' tsRNAs *in situ*

To validate RTCB-mediated ligation within the more complex cellular environment, a series of experiments were designed to extract nucleic acids from HeLa and HEK293 cells after transfection of 5' tsRNA and RTCB-mediated

ligation *in situ* and assess the formation of the ligation product. Specific detection strategies, including RT-PCR and RCA-based signal amplification, were employed to determine the presence or absence of the R-LP in cells.

5.4.1 Assessment of Transfection Efficiency

To assess the transfection efficiency, cellular distribution of synthetic 5' tsRNA-Gly^{GCC} was monitored over different time points, ranging from 2 hours to 24 hours. Both the localization and intensity of the fluorescent signals were analyzed.

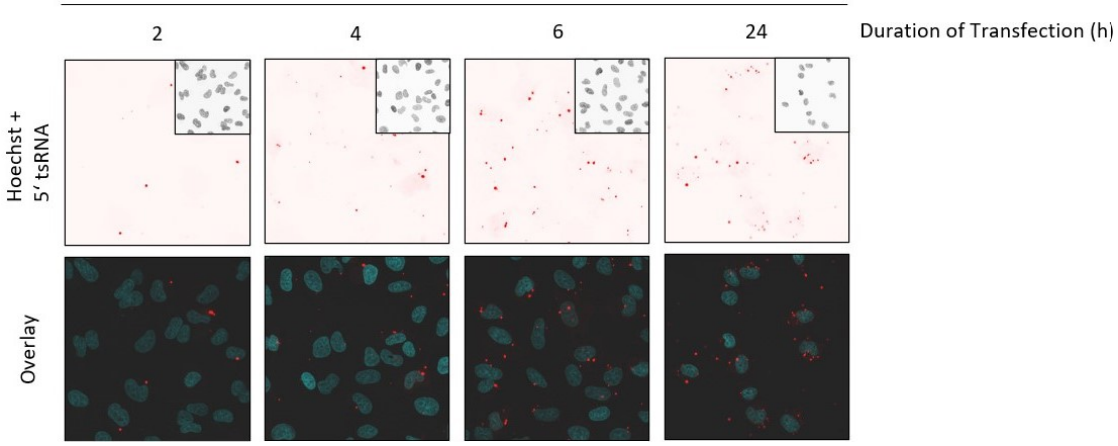

Figure 5.15: Signal intensity of fluorescently labeled 5' tsRNAs increases with increasing transfection duration.
150 ng of Atto590 (red)-labeled synthetic 5' tsRNA-Gly^{GCC} were liposomally transfected into HeLa cells using lipofectamine transfection reagent. The cells were kept in transfection media for 2, 4, 6, and 24 hours at 37°C, afterwards fixed with 4% PFA and stained for nuclei by Hoechst (blue). Analysis for localization of the transfected product by confocal microscopy followed.

The results showed that transfection of the same amount of 5' tsRNA-Gly^{GCC} resulted in similar signal localization but different signal intensity depending on the duration of transfection.

Upon examination, dot-like fluorescent patterns were observed, predominantly in the cytosol, concentrated around nuclei. At the 6-hour and 24-hour time points, the cells exhibited robust uptake and distribution of the synthetic 5' tsRNA-Gly^{GCC}. Given this, a 6-hour transfection duration was selected for further protocol optimization, as it offers sufficient cellular uptake without prolonged exposure to transfection reagents, while reducing the overall experimental time.

5.4.2 Assessment of R-LP Formation

To evaluate whether the RTCB-ligated platform (R-LP) was successfully formed following the ligation reaction in cells, two experimental approaches were used. First, HeLa cells were transfected with synthetic 5' tsRNA-Gly^{GCC} via liposomal transfection to introduce the ligation substrate. In parallel, HEK293-hANG cells were employed as a model for endogenous tsRNA generation. Upon induction with doxycycline (Dox), these cells express human angiogenin (hANG), which cleaves tRNAs, leading to the production of high numbers of endogenous 5' tsRNA-Gly^{GCC}.

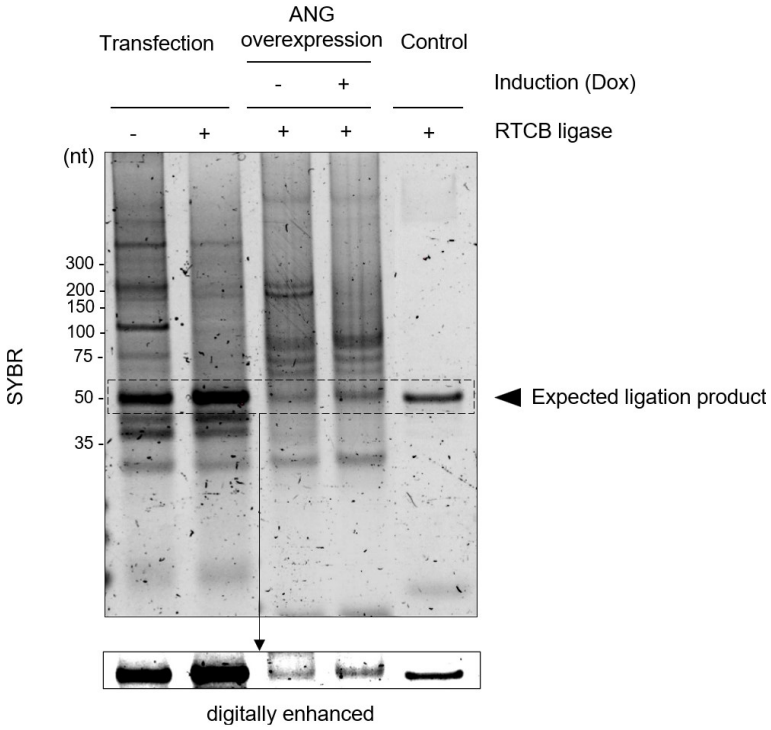

Figure 5.16: Extraction of R-LP after RTCB-mediated ligation *in situ*. Cells (10^5 cells/well) were cultured in 12-well plates. Liposomal transfection of HeLa cells was conducted using 750 ng of 5' tsRNA-Gly^{GCC} (AD137). Ectopic hANG expression in HEK293 cells was induced by Dox for 72 hours. Total RNA/DNA isolation from both HeLa and HEK293 cells following RTCB-mediated ligation was performed using Roti-Phenol extraction. RNA/DNA extracts were used as a template to perform RT-PCR. Products were expected at a size of 50 nt. As a control RTCB-mediated ligation was performed *in vitro* using 10 pmol AD137 and 10 pmol DK008. The area surrounded by a dashed window was digitally enhanced in the box below.

Following RTCB ligation reaction, total nucleic acids were extracted using phenol-chloroform to preserve potential ligation products. The presence of the R-LP was then assessed by RT-PCR using a junction-specific primer (DK017) designed to amplify the ligated product. A successful ligation was expected to

yield a defined PCR product detectable by gel electrophoresis.

However, no size shift or significant change in band intensity was observed in the RTCB-treated samples compared to the negative control lacking RTCB (Figure 5.16). This suggests that either RTCB did not access the cells or ligation products were lost during sample handling, possibly due to inefficient permeabilization or centrifugation conditions that limited RNA recovery.

Another explanation may be that ligation products were present at levels too low for RT-PCR detection. To address this, RCA-based amplification was employed as a more sensitive alternative. However, this approach also failed to yield detectable high molecular weight signals, indicating that amplification of ligation products following in situ RTCB ligation was unsuccessful (data not shown).

5.4.3 Assessment of Intracellular RTCB Localization

To assess the access and cellular distribution of exogenously introduced recombinant RTCB ligase as a prerequisite for *in situ* ligation of 5' tsRNA with hybridized CL, immunostaining was performed in HeLa cells.

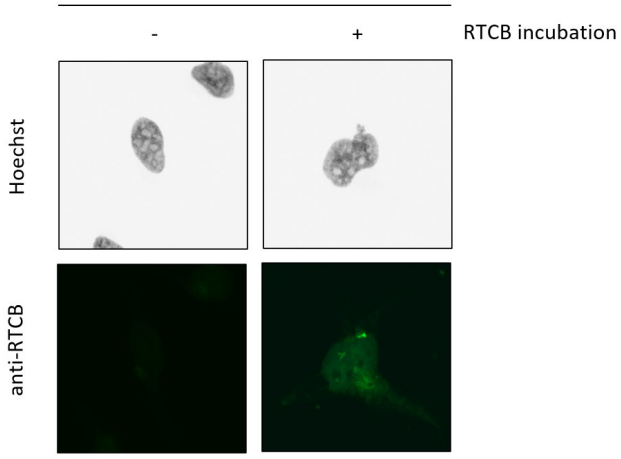

Figure 5.17: Immunofluorescence detection of exogenously introduced recombinant human RTCB ligase in HeLa cells.
HeLa cells were fixed with 4% PFA and permealbilized using 0.1% TritonX-100. Incubation with purified RTCB for 2 hours was performed, followed by staining with secondary antibody goat α-rabbit (green) bound to primary antibody rabbit α-human RTCB. Cells were stained for nuclei by Hoechst (grey). Analysis for localization of RTCB by confocal microscopy followed.

The negative control (Figure 5.17, left) showed low fluorescence, indicating the

background reactivity of the antibody. In contrast, cells incubated with recombinant RTCB (Figure 5.17, right) displayed a significantly stronger fluorescence signal, suggesting that RTCB was internalized and broadly distributed throughout the cell, rather than being confined to specific subcellular compartments.

6 Discussion

Current methodologies using sequence-specific hybridization approaches have not been successful in distinctly mapping the precise subcellular location of specific tsRNAs within cells, especially while avoiding signal detection from parental tRNAs.
However, the ability of RTCB ligase to ligate tsRNAs to complementary single-stranded DNA [35] enabled the development of an *in situ* visualization method combining RTCB-mediated ligation with RCA-based detection. The methodology's potential will be evaluated in the following three sections: biological, methodological, and technical discussion.

6.1 Biological Discussion

Considering the Low Abundance of Endogenous tsRNAs

Endogenous tsRNAs are much less abundant than their parental tRNAs, making them difficult to detect. Since tsRNAs share the same sequence as their tRNA counterparts, distinguishing them is a major challenge, especially when they make up less than 10% of the total tRNA pool in somatic cells [31, 40]. Additionally, previous studies have shown that only 1-5% of a specific tRNA isoacceptor undergoes cleavage by angiogenin (ANG) in response to stress [7]. This means that the resulting 5' tRNA are often too scarce for further biochemical analysis. Among circulating tRNA halves, glycine-derived isoacceptors are the most abundant, accounting for 46% as determined by RNA sequencing [45].
Considering this, the initial method development relied on transfection of synthetic 5' tsRNA-Gly^{GCC}, allowing for controlled testing of detection strategies before transferring findings to endogenously produced tsRNAs.

Specificity and Sensitivity of the Methodology

The specificity of the developed methodology lies in its ability to uniquely target 5' tsRNAs while excluding their parental tRNAs and other RNA fragments. This is achieved through the generation of a unique sequence during RTCB-mediated

ligation, which exploits the 3' cyclic phosphate moiety present exclusively at the ends of 5' tsRNAs. The RTCB enzyme uses this chemical feature to ligate 5' tsRNAs to a complementary linker (CL), forming a distinct RTCB-ligated platform (R-LP).
This R-LP serves as the exclusive target for the padlock probe, which is designed with a sequence complementary to the junction region of the platform. The specificity is further reinforced during padlock probe hybridization, where the probe's ends must align perfectly with the complementary sequence of the RTCB-ligated platform. Only when perfect hybridization occurs can T4 DNA ligase seal the ends of the padlock probe, generating a closed circular structure that initiates RCA.
This process inherently differentiates 5' tsRNAs from their parental tRNAs, as parental tRNAs lack the cyclic phosphate end identity required for RTCB-mediated ligation. Without the RTCB-ligated platform, the padlock probe cannot bind or be circularized, preventing RCA amplification. Thus, the methodology ensures high specificity by leveraging the unique end identity of 5' tsRNAs and requiring precise sequence complementarity during hybridization and ligation. Thereby, non-target RNAs are effectively excluded from detection.

The sensitivity of the methodology is largely driven by the principle of rolling circle amplification, which amplifies the signal from a single R-LP into a long, repetitive DNA sequence. This improves the detection signal, making it easier to visualize low-abundance 5' tsRNAs.

6.2 Methodological Discussion

Optimization of RTCB-Mediated Ligation *in vitro*

A critical step in the methodology was the RTCB-mediated ligation, which relied on the unique 3' cyclic phosphate group of 5' tsRNAs. Initial experiments aimed to optimize ligation conditions by evaluating the concentration of RTCB ligase, the cofactor GTP and reaction time. Preliminary tests revealed that increasing the GTP concentration from 0.1 mM to 0.5 mM significantly improved ligation efficiency, confirming that GTP was a limiting factor (Figure 5.5). Other studies also concluded that RTCB activity is strictly dependent on GTP, as ligation is abolished when GTP is omitted or replaced with another NTP, suggesting a guanylylation-dependent ligation mechanism [41, 46].
Archease, a known cofactor of RTCB [41, 42], was also tested to enhance ligation activity, however did not facilitate enhanced ligation efficiency when

overall reaction times were extended. Similarly, the incorporation of PEG 8000, a known stimulator of the activity of other RNA and DNA ligases [47], failed to enhance ligation efficiency using RTCB ligase under the tested conditions.

It is important to note that the presence of truncated ligation products, as revealed by Sanger sequencing, indicates that RTCB-mediated ligation may not always preserve the full 3' end of the tsRNA. However, loss of nucleotides at the ligation junction compromises the ability of the padlock probe to hybridize precisely to the expected split-landing site. As a result, this mismatch reduces the specificity of downstream targeting, since successful padlock circularization depends on perfect alignment with the ligation junction. Consequently, it is possible that truncated ligation products may cause some 5' tsRNAs to go undetected.

Targeting of R-LP *in vitro*

While optimizing ligation efficiency is critical for generating the R-LP, ensuring the structural accessibility of the platform is equally important for subsequent steps in the protocol. The "opening" of the R-LP enables targeting by the padlock probe, which is essential for initiating RCA. To achieve this structural "opening," a toehold probe was designed to hybridize with the junction region of the R-LP, the split-landing site. By binding to the complementary sequence within the linker, the toehold probe should disrupt secondary structures that may hinder padlock probe hybridization. This disruption should expose the split-landing site.
In addition to the toehold probe, the hybridization conditions, particularly the formamide concentration, played a crucial role in facilitating the "opening" of the R-LP. Formamide, a widely used denaturant, reduces the stability of RNA secondary structures [43], thereby increasing the accessibility of the ligation site for probe binding. However, tests with varying concentrations showed that there is a chance of poor target capture at too high level of stringency. As a compromise, hybridization can be done at 15% (w/v) formamide. This concentration aligns with previous studies that demonstrated its suitability for similar hybridization processes [48].

Optimization of RCA Amplification *in vitro* and *in situ*

To optimize RCA, the concentration of fluorescently labeled dUTPs was carefully adjusted to balance signal intensity and amplification efficiency (Figure 5.9). Initial tests indicated that excessive incorporation of labeled nucleotides likely

inhibited the activity of Φ29 DNA polymerase, leading to reduced amplification efficiency. This aligns with findings by Goryunova M., *et al.* [38], demonstrating that inhibition strongly depends on the structural properties of the fluorescent dye, which is integrated into the DNA strand as a part of labeled dUTP. In this thesis, a ratio of 1:10 labeled dUTP to unlabeled dTTP was identified as optimal, providing strong fluorescence signals while maintaining efficient amplification with high reaction yield.

6.3 Technical Discussion

Addressing Background Signal

Detection signals from fluorescently labeled detector probes and fluorescent nucleotide incorporation exhibited comparable background levels. Initially, fluorescently labeled dUTPs were used under the assumption that unincorporated nucleotides could be more effectively removed during washing. However, prior studies indicate that Φ29 DNA polymerase (from *Bacillus subtilis* phage) exhibits reduced efficiency when incorporating Cy3 dye-labeled dUTPs [49]. This raises concerns that Atto488 dye-labeled dUTPs might similarly impair polymerase processivity, limiting the generation of long ssDNA amplicons. While fluorescent dUTPs were effective for initial visualization, switching to detector probes yielded stronger fluorescence signals, ultimately improving the signal-to-noise ratio.

However, beyond inefficient washing, background fluorescence also arises from non-specific probe binding, including padlock probes. To address this, different padlock hybridization buffers were systematically tested. The results showed that certain compositions increased non-specific probe binding, further exacerbating background noise. Adjusting the buffer composition was thus essential for optimizing specificity while maintaining a strong signal.

Evading Fixation Artifacts

While PFA remains one of the most widely used fixatives for cellular preservation, glyoxal fixation offers the advantage of being reversible. This reversibility was considered beneficial for early method development as it may enable extraction of ligation products following RTCB-mediated ligation in cells, in order to perform further downstream experiments. PFA functions by forming covalent cross-links between proteins via methylene bridges, while glyoxal reacts primarily with amines in proteins and nucleic acids, forming weaker cross-links.

This reduced cross-linking strength can impact long-term sample stability, particularly given that glyoxal fixation is highly pH-dependent [50].
This pH sensitivity was evident in preliminary experiments, where glyoxal fixation was unstable under the alkaline conditions required for RCA-based detection, as its cross-links remain stable only at acidic pH. Consequently, tracking transfected tsRNAs after RCA-based detection revealed an altered distribution - 5' tsRNAs appeared dispersed throughout the entire cell rather than as dot-like formations localized primarily in the cytoplasm. This suggests that tsRNA accumulation was not stable following glyoxal fixation at non-optimal pH conditions. Given these limitations, glyoxal was found unsuitable as a fixative for RCA-based RNA visualization and subsequent method development proceeded using PFA.

Addressing RTCB ligase activity *in situ*

Unlike *in vitro* conditions, where ligation efficiency can be precisely controlled by optimizing buffer composition, cofactor availability, and enzyme concentration, the optimization in cells presented additional constraints. As RTCB's activity requires GTP-dependent activation [42], an imbalance - such as insufficient GTP or excess enzyme - could impair catalytic turnover or reduce substrate availability as observed in *in vitro* experiments. Optimizing this ratio is therefore essential to ensure that the enzyme remains active and that ligation proceeds efficiently under the complex conditions of the cellular environment.

Another concern was the accessibility of ectopically introduced RTCB to its substrate. However, immunostaining confirmed that RTCB successfully entered the cell post-fixation, indicating that its localization might not be the primary limiting factor. Given that it is distributed throughout the cytoplasm, RTCB can be assumed to be available for interactions with 5' tsRNAs and complementary linker oligonucleotides.

Nevertheless, ligation efficiency may still be compromised by steric hindrance from cellular proteins obstructing the ligation site or by the hydrolysis of the cyclic phosphate following transfection. If cycP is lost or blocked before ligation, the reactive group necessary for RTCB activity would no longer be available.

6.4 Summary and Outlook

The findings of this thesis demonstrate that RTCB ligase can covalently link specific tsRNAs to complementary linkers, differentiating them from their mature tRNAs. While ligation was successfully validated *in vitro*, its efficiency in cells might be the main obstacle that limited the success of *in situ* ligation attempts.

To enhance signal detection, this study combined RTCB-mediated ligation with rolling circle amplification (RCA) as a method for selectively and sensitively detecting specific tRNA fragments. RCA-based detection was validated *in vitro* and showed promise *in situ*, suggesting its suitability for *in situ* detection of low abundant tsRNAs in mammalian cells after their ligation to a linker. However, further optimizations may be needed to adapt the detection methodology from synthetic analogs to endogenous tsRNAs.

Bibliography

1. Palazzo, A. F. & Lee, E. S. Non-coding RNA: What is functional and what is junk? *Front. Genet.* **5** (2015).
2. Li, S., Xu, Z. & Sheng, J. tRNA-derived small RNA: A novel regulatory small non-coding RNA. *Genes* **9,** 246 (2018).
3. Dhahbi, J. *et al.* Profiling of tRNA Halves and YRNA Fragments in Serum and Tissue From Oral Squamous Cell Carcinoma Patients Identify Key Role of 5 tRNA-Val-CAC-2-1 Half. *Front. Oncol.* **9,** 959 (2019).
4. Peng, H. *et al.* A novel class of tRNA-derived small RNAs extremely enriched in mature mouse sperm. *Cell Res.* **22,** 1609–1612 (2012).
5. Srinivasan, S. *et al.* Small RNA Sequencing across Diverse Biofluids Identifies Optimal Methods for exRNA Isolation. *Cell* **177,** 446–462.e16 (2019).
6. Lee, S. R. & Collins, K. Starvation-induced cleavage of the tRNA anticodon loop in Tetrahymena thermophila. *J. Biol. Chem.* **280,** 42744–42749 (2005).
7. Yamasaki, S., Ivanov, P., Hu, G. F. & Anderson, P. Angiogenin cleaves tRNA and promotes stress-induced translational repression. *J. Cell Biol.* **185,** 35–42 (2009).
8. Oberbauer, V. & Schaefer, M. R. tRNA-derived small RNAs: Biogenesis, modification, function and potential impact on human disease development. *Genes* **9,** 607 (2018).
9. Fu, H. *et al.* Stress induces tRNA cleavage by angiogenin in mammalian cells. *FEBS Letters* **583,** 437–442 (2009).
10. Schutz, K., Hesselberth, J. R. & Fields, S. Capture and sequence analysis of RNAs with terminal 2,3- cyclic phosphates. *RNA* **16,** 621–631 (2010).
11. Honda, S., Morichika, K. & Kirino, Y. Selective amplification and sequencing of cyclic phosphate-containing RNAs by the cP-RNA-seq method. *Nat. Protoc.* **11,** 476–489 (2016).

12. Shen, Y. *et al.* Transfer RNA-derived fragments and tRNA halves: biogenesis, biological functions and their roles in diseases. *J. Mol. Med.* **96,** 1167–1176 (2018).

13. Haussecker, D. *et al.* Human tRNA-derived small RNAs in the global regulation of RNA silencing. *RNA* **16,** 673–695 (2010).

14. Green, J. A., Ansari, M. Y., Ball, H. C. & Haqqi, T. M. tRNA-derived fragments (tRFs) regulate post-transcriptional gene expression via AGO-dependent mechanism in IL-1 stimulated chondrocytes. *Osteoarthr. Cartil.* **28,** 1102–1110 (2020).

15. Fu, B. F. & Xu, C. Y. Transfer RNA-Derived Small RNAs: Novel Regulators and Biomarkers of Cancers. *Front. Oncol.* **12,** 843598 (2022).

16. Gapp, K. *et al.* Implication of sperm RNAs in transgenerational inheritance of the effects of early trauma in mice. *Nat. Neurosci.* **17,** 667–669 (2014).

17. Alata-Jimenez, N. *et al.* Paternal methotrexate exposure affects sperm small RNA content and causes craniofacial defects in the offspring. *Nat. Commun.* **14,** 1617 (2023).

18. Jin, F. *et al.* A novel class of tsRNA signatures as biomarkers for diagnosis and prognosis of pancreatic cancer. *Mol. Cancer* **20** (2021).

19. Zhou, K. *et al.* A tRNA fragment, tRF5-Glu, regulates BCAR3 expression and proliferation in ovarian cancer cells. *Oncotarget* **8,** 95377–95391 (2017).

20. Pekarskya, Y. *et al.* Dysregulation of a family of short noncoding RNAs, tsRNAs, in human cancer. *Proc. Natl. Acad. Sci. USA* **113,** 5071–5076 (2016).

21. Martinez, B. V. *et al.* Circulating small non coding RNA signature in head and neck squamous cell carcinoma. *Oncotarget* **6,** 19246–19263 (2015).

22. Telonis, A. G. *et al.* TRNA fragments show intertwining with mRNAs of specific repeat content and have links to disparities. *Cancer Res.* **79,** 3034–3049 (2019).

23. Blanco, S. *et al.* Aberrant methylation of t RNA s links cellular stress to neuro-developmental disorders. *EMBO J.* **33,** 2020–2039 (2014).

24. Schaffer, A. E. *et al.* CLP1 founder mutation links tRNA splicing and maturation to cerebellar development and neurodegeneration. *Cell* **157,** 651–663 (2014).

25. Hori, H. Methylated nucleosides in tRNA and tRNA methyltransferases. *Front. Genet.* **5** (2014).

26. Liapi, E., van Bilsen, M., Verjans, R. & Schroen, B. tRNAs and tRNA fragments as modulators of cardiac and skeletal muscle function. *Biochim. Biophys. Acta, Mol. Cell Res.* **1867,** 118465 (2020).

27. Xie, Y. *et al.* Action mechanisms and research methods of tRNA-derived small RNAs. *Signal Transduct Target Ther.* **5** (2020).

28. Shaffer, S. M., Wu, M.-T., Levesque, M. J. & Raj, A. Turbo FISH: A Method for Rapid Single Molecule RNA FISH. *PLoS ONE* **8,** e75120 (2013).

29. Gall, J. G., Lou, M., Kline, P. & Giles, N. H. Formation and detection of RNA-DNA hybrid molecules in cytological preparations. *Proc. Natl. Acad. Sci. U.S.A.* **63,** 378–383 (1969).

30. Hauptmann, G., Söll, I., Krautz, R. & Theopold, U. Multi-target chromogenic whole-mount In Situ hybridization for comparing gene expression domains in Drosophila embryos. *J. Vis. Exp.* **107** (2016).

31. Li, J. *et al.* Rolling circle extension-assisted loop-mediated isothermal amplification (Rol-LAMP) method for locus-specific and visible detection of RNA N6-methyladenosine. *Nucleic Acids Res.* **51,** e51–e51 (2023).

32. Zhuang, P. *et al.* Combined microRNA and mRNA detection in mammalian retinas by in situ hybridization chain reaction. *Sci. Rep.* **10** (2020).

33. Tsuneoka, Y. & Funato, H. Modified in situ Hybridization Chain Reaction Using Short Hairpin DNAs. *Front. Mol. Neurosci.* **13** (2020).

34. Tian, W., Li, P., He, W., Liu, C. & Li, Z. Rolling circle extension-actuated loop-mediated isothermal amplification (RCA-LAMP) for ultrasensitive detection of microRNAs. *Biosens. Bioelectron.* **128,** 17–22 (2019).

35. Borac, L. *Establishment of a fluorescence in situ hybridization-based methodology for the visualization of specific tRNA-derived fragments* (2021).

36. Takahashi, H. *et al.* Direct detection of mRNA expression in microbial cells by fluorescence in situ hybridization using RNase H-assisted rolling circle amplification. *Sci. Rep.* **10** (2020).

37. Berr, A. & Schubert, I. Direct labelling of BAC-DNA by rolling-circle amplification. *Plant Journal* **45,** 857–862 (2006).

38. Goryunova, M., Arzhanik, V., Zavriev, S. & Ryazantsev, D. Rolling circle amplification with fluorescently labeled dUTP-balancing the yield and degree of labeling. *Analytical and Bioanalytical Chemistry* (2006).

39. Lin, C., Xiao, Z., Zhang, X. & Wu, G. In situ hybridization assay for circular RNA visualization based on padlock probe and rolling circle amplification. *Biochemical and Biophysical Research Communications* **610,** 30–34 (2022).

40. Drino, A. *et al.* Production and purification of endogenously modified tRNA-derived small RNAs. *RNA Biology* **17,** 1104–1115 (2020).

41. Popow, J., Jurkin, J., Schleiffer, A. & Martinez, J. Analysis of orthologous groups reveals archease and DDX1 as tRNA splicing factors. *Nature* **511,** 104–107 (2014).

42. Gerber, J. L. *et al.* Structural and mechanistic insights into activation of the human RNA ligase RTCB by Archease. *Nat. Commun.* **15** (2024).

43. Hoyos-Manchado, R. *et al.* RNA metabolism is the primary target of formamide in vivo. *Sci. Rep.* **7** (2017).

44. Krzywkowski, T., Hauling, T. & Nilsson, M. In Situ Single-Molecule RNA Genotyping Using Padlock Probes and Rolling Circle Amplification. *Methods Mol. Biol. (Clifton, N.J.)* **1492,** 59–76 (2017).

45. Dhahbi, J. M. *et al.* 5 tRNA halves are present as abundant complexes in serum, concentrated in blood cells, and modulated by aging and calorie restriction. *BMC Genomics* **14** (2013).

46. Tanaka, N., Chakravarty, A. K., Maughan, B. & Shuman, S. Novel mechanism of RNA repair by RtcB via sequential 2,3- cyclic phosphodiesterase and 3-phosphate/5-hydroxyl ligation reactions. *J. Biol. Chem.* **286,** 43134–43143 (2011).

47. Harrison, B. & Zimmerman, S. B. Polymer-stimulated ligation: enhanced ligation of oDgo-and polynudeotides by T4 RNA bgase in polymer solutions. *Nucleic Acids Res.* **12** (1984).

48. Yilmaz, L. S., Loy, A., Wright, E. S., Wagner, M. & Noguera, D. R. Modeling formamide denaturation of probe-target hybrids for improved microarray probe design in microbial diagnostics. *PLoS ONE* **7** (2012).

49. Smolina, I. V. *et al.* High-density fluorescently labeled rolling-circle amplicons for DNA diagnostics. *Anal. Biochem.* **347,** 152–155 (2005).

50. Richter, K. N. *et al.* Glyoxal as an alternative fixative to formaldehyde in immunostaining and super-resolution microscopy. *EMBO J.* **37,** 139–159 (2018).

List of Figures

List of Tables